FIRST GUESS DEPENDENCE OF PHYSICALLY BASED

TEMPERATURE-HUMIDITY RETRIEVALS FROM HIRS2/MSU DATA

J. Susskind and D. Reuter
Goddard Laboratory for Atmospheres
Code 611
NASA/Goddard Space Flight Center
Greenbelt MD 20771

and

Andrew Pursch
Sigma Data Services Corp.

## 1. INTRODUCTION

Physical retrievals of temperature and humidity profiles from atmospheric sounders such as HIRS2/MSU have a number of advantages over purely statistical approaches. Most significantly they allow directly for the incorporation of factors affecting the radiances, other than atmospheric temperature humidity profiles, such as surface properties, zenith angle of observation, and most important of all, clouds. As shown in Susskind et al., 1984, the GLA (formerly called GLAS) physical retrieval scheme produces temperature fields which do not degrade appreciably with increasing cloudiness. In addition, the analysis method allows for determination of surface properties and cloud fields from the data.

Another advantage of physical retrievals is the ability to incorporate first guess information into the retrieval process. This is potentially helpful information if the first guess is good and potentially harmful information if the first guess is poor. A good retrieval scheme should have the property that significant changes can be made to improve a very poor first guess but only minor changes should be made to an excellent first guess. Indeed, a question often asked about physical retrievals utilizing a first guess is how much of the result comes from data and how much from the guess.

In this study, temperature humidity retrievals over the ALPEX region were done for two successive overpasses of NOAA 7 on roughly March 4 12Z and March 5 0Z 1982. This period was characterized by a rapidly changing synoptic situation with a sharp trough moving to the east. Three sets of retrievals were done for each synoptic period using different initial guess fields. The first initial guess field was a 24 hour lagged NMC analysis, which is an extremely poor representation of the actual synoptic situation. The second initial guess field was the NMC analysis at the closest synoptic time to the flight overpass, which might be taken as "almost truth", the almost arising both because the analysis is not perfect and because of a time difference between the satellite overpasses and the analysis time. The third guess was a forecast for the region made from an analysis guess 6 hours

hours earlier using the GLA forecast analysis system (Baker et al.,1984). This guess is the same as that used routinely in the GLA processing of global fields from HIRS2/MSU data.

Ideally, the three sets of results should look very much like each other and like the concurrent NMC analysis, while representing a significant improvement over the lagged analysis first guess and perhaps a minor improvement over the six hour forecast. One does not expect the three sets of retrievals to be identical, for that would mean that the retrievals are totally independent of the guess.

The temperature retrievals are done in a manner very similar to that described in Susskind et al. (1984). Modifications to the system as well as results comparing the thickness fields, will be described in the next section. The humidity retrieval algorithm, which has been recently developed, together with the results comparing the humidity fields, will be shown in the third section.

The humidity retrievals at this point are done subsequent to the temperature retrievals, that is, the retrieved temperature profiles influence the results of the humidity retrievals, but the retrieved humidity profiles do not influence the retrieved temperature profiles. The first guess relative humidity profile is held constant during the temperature analysis. This does not have a major effect on the retrieved temperature profiles but does introduce a subtle first guess dependence which might be reduced (or amplified) if the modified relative humidities are allowed to affect the temperature retrievals. Research on this will be done in the future.

## 2.1 Determination of atmospheric temperature profiles

The retrievals of atmospheric and surface temperatures were done almost exactly as in Susskind et al. (1984) with three exceptions, retrieval density, cloud filtering algorithm, and rejection criterion. Retrievals for this study were run one retrieval per 4 x 4 array of HIRS2 spots. This array was broken into four 2 x 2 spot sub-arrays each divided into two "fields of view" constructed by averaging the radiances for each channel for the two spots with the largest 11 µm window radiances, called field of view 1, and with the smallest 11 µm window radiances, called field of view 2. This is the finest resolution with which we feel HIRS2 retrievals can be done. One retrieval can be done in each of the four sub-arrays. In this study, only one retrieval was done in a 4 x 4 array of spots, located in the 2 x 2 sub-array containing the highest 11 µm window field of view radiance in the array. The closest MSU spot to the center of the sub-array was taken to be representative of the measurement for the sub-array. No interpolation of MSU radiances was done because of the large zenith angle dependence of the MSU observations.

Given radiances for fields of view 1 and 2 in a sub-array, $R_{i,1}$ and $R_{i,2}$, clear column radiances for channel i, $\tilde{R}_i$ are reconstructed, much as in Susskind et al. (1984), according to

$$\tilde{R}_i = R_{i,1} + \eta(R_{i,1} - R_{i,2}) \quad (1)$$

where $R_{i,1}$ is the observed radiance for channel i in the field of view having the larger 11 μm radiance, and $R_{i,2}$ is the observation of channel i in the second field of view. If $R_{i,CLR}$ is known for a given channel, then η can be solved for according to

$$\eta = \frac{R_{i,CLR} - R_{i,1}}{R_{i,1} - R_{i,2}} \quad (2)$$

Since $\eta = \alpha_1/(\alpha_1 - \alpha_2)$, it should not be dependent on the channel used. In Susskind et al. (1984), η was determined by combined use of HIRS2 channel 13 and MSU channel 2. $R^N_{13,CLR}$ is computed in each iteration (N) using the Nth iterative temperature profile and ground temperature. If the $N^{th}$ guess is too warm (or cold), $R^{(N)}_{i,CLR}$ would be too large (or small). The effect on the computed brightness temperature of channel 13 of a bias in the temperature profile in the troposphere is accounted for, to first order, by modifying the brightness temperature according to

$$\theta'_{13} = \theta^N_{13,CLR} + \theta_{M2} - \theta^N_{M2} \quad (3)$$

where $\theta^N_{13,CLR}$ is the equivalent brightness temperature to $R^N_{13,CLR}$, $\theta_{M2}$ is the observed brightness temperature in MSU channel 2, which is sensitive to the average tropospheric temperature, and $\theta^N_{M2}$ is the computed computed brightness temperature in MSU channel 2. This procedure works reasonably well even though channel 13 is sensitive primarily to radiation mcuh closer to the surface than that of MSU channel 2. $\eta_{13}$ is then computed according to

$$\eta_{13} = \frac{B_{13}[\theta'_{13}] - R_{13,1}}{R_{13,1} - R_{13,2}} \quad (4)$$

where $B(\theta')$, the black body function of the corrected equivalent brightness temperature, is the corrected estimate of the clear column radiance. While results using equations (1-4) are quite good, it has been found that in cases where the initial guess has a lapse rate error, improved results are obtained by defining $\eta_{14}$ in an analogous manner to $\eta_{13}$ in equations (3) and (4) and setting η equal to the average of $\eta_{13}$ and $\eta_{14}$ weighted by the square of the difference in radiances for each channel in each field of view:

$$\eta = \frac{\eta_{13}(R_{13,1}-R_{13,2})^2 + \eta_{14}(R_{14,1}-R_{14,2})^2}{(R_{13,1}-R_{13,2})^2 + (R_{14,1}-R_{14,2})^2} \quad (5)$$

Including channel 14 radiances in the determination of η has the effect of utilizing a single infra-red channel with a broader weighting function, more in line with that of the microwave channel, to correct for cloud effects. Combined use of channels 13 and 14 was especially necessary for NOAA 7 data because the weighting functions for both channels 13 and 14 were shifted lower in the atmosphere relative to TIROS-N and channel 13 provided an even poorer match with MSU channel 2. The procedure gives improved results with TIROS-N data as well.

In Susskind et al. (1984), retrievals were rejected as non-convergent if either 1) R, the root mean square difference between the reconstructed brightness temperatures for the seven temperature sounding channels (HIRS2 channels 2, 4, 13, 14, and 15, and MSU channels 3 and 4) and the brightness temperatures computed for these channels using the solution, is greater than 1°C or 2) D, the absolute difference between the observed and computed brightness temperature for MSU channel 2, is greater than 1°C. In the region of this study, it was found that many differences for MSU channel 2 were greater than 1°C but the retrievals still looked reasonable when R was small. Therefore, a new more flexible criterion was used, involving the sum of the two quantities R and D. The retrieval was accepted and called good quality if R + D was less than 1.8°C, was called fair quality if R + D was between 1.8°C and 2.3°C, and poor quality if R + D was between 2.2°C and 2.8°C. Retrievals were rejected if R + D was greater than 2.8°C. These quality indicators were written on the tapes sent to the workshop. In constructing the fields shown in the next section, all accepted retrievals were weighted equally. Retrievals rejected because of the above criterion or others such as the scene being too cloudy to perform an infrared retrieval ($\eta$>4) were not included in the analyses. No "microwave only retrievals" are performed.

## 2.2 First guess dependence of atmospheric thicknesses

Figures 1-10 show local analyzed fields for a number of thicknesses at times corresponding roughly to March 4, 1982 12Z and March 5, 1982 0Z. Each figure contains three analyses based only on quantities derived from satellite retrievals using as a first guess the concurrent NMC analysis, the 24 hour lagged analysis and a 6 hour forecast based on the GLAS GCM. The analyses based on the retrievals are shown in panels (A), (C) and (E). The analyses based on the first guess fields themselves are shown in panels (B), (D), and (F). In the case of satellite retrievals, data is included in the analysis only in locations where acceptable retrievals were performed. The first guess fields include data at all grid points (4° x 5°) in the area. The only information used in generating the retrievals, aside from topography and climatological sea surface temperatures, was the observed radiances, which are identical in all three sets of retrievals, and the first guess temperature-humidity profiles and surface pressure, which is different. No surface analysis or other concurrent measurements are used which are not shown in the guess field.

Figures 1-5 show the 700-1000 mb thickness, the 500-1000 mb thickness, the 500 - 700 mb thickness, the 300 - 500 mb thickness, and the 100 - 300 mb thickness for the March 4 12Z time period. The satellite retrievals are based on two orbits crossing at about 1330Z in the center and west and 1200Z in the east. No attempt was made to account for the time difference in computing the satellite analysis. For the purpose of this comparison, we may consider panel (B), the concurrent NMC analysis, as the truth. It is clear by comparing figures 1-5(B) with 1-5(D) that the 24 hour lagged analysis guess was grossly different at all levels. The 6 hour forecast guess shown in figures 1-5(F) is in general much closer to the analysis, as might be expected, but significant differences exist.

Figures 6-10 show the same fields for the time period March 5 00Z. In this case, the satellite overpasses were at 0200Z in Eastern Europe and about 0345Z in the west and central portions of the field . Here, differences between retrievals and analysis fields may be real, due to the 2-4 hour time difference and the rapidly moving field. As in figures 1-5, the 24 hour lagged analysis guess is grossly different from the true field while the 6 hour forecast is similar, but not identical, to the analysis.

It is of interest to compare the three sets of retrievals with each other for consistency and with the analysis for accuracy. The three sets of retrievals are in general much closer to each other than the guesses are to each other, and also show good agreement compared to the analyis. In figure 2, showing 500 - 1000 mb thickness, for example, the analysis shows a moderate trough with north-south orientation centered at about 2°W longitude, and a ridge with north-east, south-west orientation running roughly through 10°W, 30°N and 20°E, 42°N. These main features are found with slightly varying degrees of intensity in all the fields shown, with the exception of the 24 hour lagged analysis, which is almost 180° out of phase. It is apparent then that in this thick layer, the retreivals are relatively first guess independent and can significantly improve a poor guess while not degrading a good guess. The same basic result holds for the 700-1000 mb thickness field and the 500-700 mb thickness field as well. In the latter field, the gradient in the trough in the retrieved field using the lagged analysis guess is somewhat weaker than in the other retrieved fields or in the analysis. It is also interesting to note that in this field, the retreival from the forecast guess gives a better depiction of the intensity and shape of the trough, as compared to the analysis, than does the forecast guess. This indicates some guess dependence but also the ability to improve on a 6 hour forecast which is already fairly accurate. The upper level thicknesses, 300-500mb and 100-300 mb, also show similar findings. Again, all retrievals fields show the same patterns as each other and the analysis, but the gradients are somewhat weaker, expecially in the 100-300 mb thickness field when an extremely poor first guess is used.

By March 5 0Z, the center of the trough at 500 mb has moved about 5° further east and deepened. The 6 hour forecast has the trough centered about 7° too far west. The 24 hour lagged analysis, as in the earlier period, shows a totally different synoptic situation. The findings with regard to guess dependence as a function of layer are basically the same as in the previous period. The differences between the retrievals at the lower atmospheric levels, 700 - 1000 mb and 500 - 1000 mb, are very small. At the higher levels, the retrieved features all are again very similar to each other and the concurrent analysis, but the gradients are weakened somewhat with the poorer first guesses.

It is extemely interesting to note in figure 7, the 500 - 1000 mb thickness for March 5 0Z, that all retreival fields have the trough centered at about 5°E, while the concurrent analysis has the trough centered at 2°E, the forecast at 2°W, and the lagged analysis at about 10°W. The location of the satellite retreived trough 3° east of the analysis trough may well be a real effect due to movement in time. The same result is found in the 700-1000 mb and 500-700 mb thickness fields. Perhaps the most striking result is in the 100-300 mb thickness field for March 5 0Z. Here figures 10(C) and 10(D) both show highly structured fields with large gradients that are totally different from one another. All retreivals show a closed high centered at about 44°N, 5°E and a closed low at about 44°N, 22°E, in good agreement with the analysis. The sharp gradients around the high are not found in the forecast guess and the lagged analysis contains a low in this area. This figure clearly shows the degree to which satellite data can improve upper air analysis, though the gradients are weaker than reality in the case of a very bad guess.

## 3.1 Humidity Retrieval Algorithm

The method used for retrieving atmospheric water vapor profiles is similar to that used for the temperature retrievals, in that heavy reliance is placed on the ability to accurately model the response of a given channel to changes in atmospheric water vapor, as opposed to using statistical relationships between brightness temperature and water vapor content. It should be noted that the effect of changes of water vapor on those channels most sensitive to water vapor content, channels 8, 10, 11, and 12 on the HIRS instrument, is somewhat different than the effect of temperature changes on the temperature sounding channels. In the latter case, the change in observed radiance is due primarily to changes in the Planck function in the radiative transfer equation, while the former case the radiance change is due mainly to changes in the transmittance function. In other words, for the temperature sounding channels the weighting functions are relatively insensitive to moderate changes in temperature, while for a humidity sounding channel the major effect of a change in water vapor profile is to alter the region of the atmosphere which is probed by the channel. Because of this, accurate water vapor distributions may only be obtained if the atmospheric temperature profile is well determined. Therefore, in the method to be described below, the humidity retrieval is performed after the temperature retrieval.

The iterative relaxation method for determination of atmospheric water vapor proceeds in the following steps:

1) Given the retrieved atmospheric and surface temperatures and a first guess water vapor distribution, $q^0(P)$, the brightness temperature, $\Theta_i^c$, which would be expected to be observed in a given channel may be calculated from the radiative transfer equation. The first guess will be modified according to the difference between $\Theta_i^c$ and $\tilde{\Theta}_i$, the reconstructed (observed) brightness temperature and the sensitivity of $\Theta_i^c$ to changes in humidity.

2) In order to estimate the sensitivity of brightness temperatures to humidity changes, the entire guess water vapor profile is alternately increased and decreased by a fixed fraction $\delta$ and estimates of the brightness temperature are obtained for each case, for each channel to be used in the retrieval. The change in brightness temperature in channel i for a fractional change in water vapor of $\pm\ \delta$ is approximated as

$$\Delta\Theta_i^c \pm \ = \ \Theta_i^c\ [q^N(P)] - \Theta_i^c\ [q^N(P)\cdot(1 \pm \delta)] \qquad (6)$$

3) Each channel i then provides an estimate of the fractional change to be made in humidity, $f_i$, computed according to

$$f_i = \left(\frac{\tilde{\Theta}_i - \Theta_i^c}{\Delta\Theta^c_{i\pm}}\right)\delta \qquad (7)$$

where $\Delta\Theta^c_{i+}$, the estimate of sensitivity to increasing humidity, is used if the computed brightness temperature is too high, in which case f is taken as positive, and $\Delta\Theta^c_{i-}$ is used otherwise, resulting in a negative $f_i$. Because the problem is nonlinear, $|f_i|$ is never allowed to be greater than 0.7 in any iteration.

4) Since each channel senses a different region of the atmosphere, the 4 estimates of $f_i$ will not be the same in general. A fractional change, $\varepsilon\ (P_j)$ must be found at each of the n discrete pressure levels used in modeling the radiative transfer equation. This is done by weighting the values of $f_i$ according to

$$\varepsilon\ (P_j) = \sum_i W_i\ (P_j) f_i / \sum_i W_i\ (P_j) \qquad (8)$$

where $W_i\ (P_j)$ represents the relative sensitivity of channel i to humidity changes at $P_j$. In these calculations, $W_i(P_j)$ was approximated by the analog of the temperature sounding weighting function

$$W_i(P_j) = \left(\frac{d\tau_i}{d\ell np}\right)_{P_j} / (1 - \tau(P_s)) \qquad (9)$$

which is easier to compute than the actual sensitivity function relating changes in brightness temperatures to changes in humidity at specific levels, and provides essentially identical soudings. Equation 8 is evaluated discretly at mid-mandatory levels and the values of $\varepsilon\ (P_j)$ are linearly interpolated in P at intermediate values.

5) Using the values of $\varepsilon(P)$ determined in step 4, a new estimate of the water vapor profile at the n discrete pressure levels is found as

$$q^{N+1}(P) = q^{N}(P)(1+ \varepsilon(P)) \quad . \qquad (10)$$

If, for any level, $q^{N+1}(P)$ is found to correspond to a relative humidity of greater than 100%, then for that level $q^{N+1}(P)$ is set to the value of the specific humidity which corresponds to 100% relative humidity. Furthermore, because of the limited sensitivity of the infrared brightness temperatures to changes in water vapor near the surface, the values of $\varepsilon(P)$ beneath the mandatory level pressure closest to the surface are set to the value of $\varepsilon(P)$ at that mandatory level. This profile is used to obtain new values for the atmospheric transmittances for the 4 channels which are then used to calculate new estimates of the brightness temperatures $\Theta_i^c[q^{N+1}(P)]$. If the residuals between $\tilde{\Theta}_i^c[q^{N+1}(P)]$ and $\Theta_i$ are sufficiently small, or if there is little change in the residuals, the process is considered to have converged and $q^{N+1}(P)$ is taken to be the retrieved water vapor profile. If this is not the case, steps 2 through 5 are repeated. Currently the process is limited to at most seven iterations.

There are some exceptions to this procedure in actual practice. For example, if a temperature retrieval is not performed for any reason, or, if the temperature retrieval is flagged as nonconvergent, then no water vapor retrieval is performed. Furthermore if the sensitivity of a given channel to changes in water vapor content, as defined in step 2 above, is too small, then that channel is not used in the retrieval process. This is accomplished by setting $W_i(P) = 0$ for the channel. This situation arises occasionally for channels 8 and 10 which sense near the surface where there is sometimes little thermal contrast. Indeed, for an isothermal atmosphere and a surface with unit emissivity, a passive sounding has no information about water vapor content.

After a full iterative cycle has been performed, the residual differences between the observed and calculated brightness temperatures may be used to reject a retrieved profile. At the present time only a very gross check is done and a water vapor retrieval is rejected if the rms of the residuals of channels 11 and 12 is more than 2° or if the absolute value of the residual of either channels 8 or 10 is more than 5°. A looser criterion is used for these channels because they are affected by uncertainties in ground temperature and surface emissivity. If, as described above, either channel 8 or 10 is not used in the retrieval process, the residual is allowed to be 10° before the profile is rejected. As with the thickness fields shown previously, the retrieved fields shown in the next section contain only accepted retrievals while the first guess fields contain first guess humidities at all locations.

## 3.2 First guess dependence of humidity retrievals

Figures 11-16 A-F show the precipitable water above 1000 mb (actually above the surface), 700 mb and 500 mb and dewpoints at 850 mb, 700 mb and 500 mb for the retrieval and first guess fields for March 4 12Z. Analogous fields for March 5 0Z are shown in figures 17-22 A-F. In the case of thickness retrievals, it was found that all retrievals produced very similar fields to each other and to the concurrent analysis, with the largest first guess sensitivity coming at the higher levels of the atmosphere, for which the vertical resolution of HIRS/MSU is poorest. A very different result is obtained for the humidity retrievals, in which retrieved fields are more different from each other, and especially from the analysis. Furthermore, the guess dependence for humidity retrievals is greatest closer to the surface. The larger guess dependence for humidity retrievals occurs because the HIRS2 observations are not as sensitive to changes in humidity, especially close to the surface, as they are to changes in temperature, and the vertical resolution of the humidity sounding channels is poor. The poorer agreement of retreivals with the NMC humidity analysis is partially due to this decreased sensitivity in the retrievals. Another factor is that the analysis is itself of poorer quality than the thickness analysis and therefore cannot necessarily be taken as truth. While verification is difficult and sensitivity is relatively poor, there is no question that useful information is present, especially at 500 mb.

Figure 13 A-F shows the precipitable water above 500 mb at March 4 12Z constructed from the three first guesses and the three sets of retrievals. The NMC analysis shows a moist tongue running northeast diagonally through the scene with the northeast containing the most moisture. The twenty-four hour lagged analysis is considerably more moist, with the moist line having the same orientation but shifted toward the northwest. The six hour forecast from the GLA GCM looks quite different from the NMC analysis, as it will in all cases. In this case, the forecast field is characterized by two moist centers in its northeast and southeast corners. It is pleasing to see that all retrievals are generally similar in structure to each other and to the NMC analysis, though they all tend to have more precipitable water above 500 mb than the analysis. This bias may be a real error or it may be due to an underestimate of precipitable water above 500 mb by the analysis, in which humidity information above 500 mb is sparse. All retrievals also tend to show an increase in humidity at the southeast corner of the field though less so than in the forecast guess.

The general features in the precipitable water above 700 mb and above 1000 mb field in figures 11 and 12 are similar to those in the upper level humidity field, though the first guess dependence, and the difference between the fields, increases with increasing reference pressure. Note for example that the precipitable water above 1000 mb fields in figures 11 C and D show an extremely moist first guess field in the northwest quadrant which was corrected somewhat in the retrieval, but is still moist compared to the other retrievals. Likewise, the central area of the field is considerably more moist in figure 10E, reflecting the moist guess in figure 10F, than in other fields. The results are more clearly depicted in the retrieved dewpoint fields (figures 14-16) which do not show major differences at 500 mb but show significant differences at 850 mb in the northwest corner, where a very dry forecast first guess (figure 14F) was left virtually unchanged in the retrieval (figure 14E).

At March 5 0Z, the precipitable water above 500 mb (figure 19) is characterized by a dry area centered about 4° E with increasing moisture on either side, particularly over central Italy and to the northeast. The first guess fields are all rather different while the retrievals generally share the same characteristics. The six hour forecast field appears to be the biggest outlier and it was corrected appreciably by the retrieval if the analysis is taken as truth. The retrieved precipitable water above 700 mb fields (figure 18) are again similar to each other but contain a moist area centered about 42 N, 6W, which is not evident in any guess field. The largest differences between retrieval fields again occurs in the precipitable water above 1000 mb fields (figure 17), where the forecast field is particularly dry in the southwest corner and this dry area is again reflected in the retrieval. Likewise, the 24 hour lagged analysis guess is too dry over Italy and little was done to correct this in the retrieval field. The differences are more apparent in the dew point fields in which the retrieved results are basically similar at 500 mb but show major differences at 850 mb.

## 4. CONCLUSIONS

It has been demonstrated that the method described in Susskind et al. (1984) for atmospheric temperature retrievals, results in a very low first guess dependence for retrieved thickness fields, which is smallest close to the surface, and increases at higher levels, where the weighting functions of HIRS2/MSU are not as sharp. A poor first guess is changed and improved considerably whereas an accurate first guess is not degraded. No surface informaton was used in the retrieval process.

The situation for humidity retrievals, as performed in this paper, is somewhat less ideal. A larger first guess dependence is observed, especially close to the surface, where the radiances are less sensitive to changes in humidity. On the other hand, there is evidence that a poor first guess can be improved upon, especially in the mid-troposphere, though there is a question as to what constitutes "truth".

## References

Baker, W. E., R. Atlas, M. Halem, and J. Susskind, 1984: A Case Study of Forecast Sensitivity to Data and Data Analysis Techniques. Mon. Wea. Rev., 112, 1544-1561.

Susskind, J., J. Rosenfield, D. Reuter, and M. T. Chahine, 1984: Remote Sensing of Weather and Climate Parameters from HIRS2/MSU on TIROS-N. J. Geophys. Res., 89, 4677-4697.

# 700–1000 MB THICKNESS MARCH 4, 1982

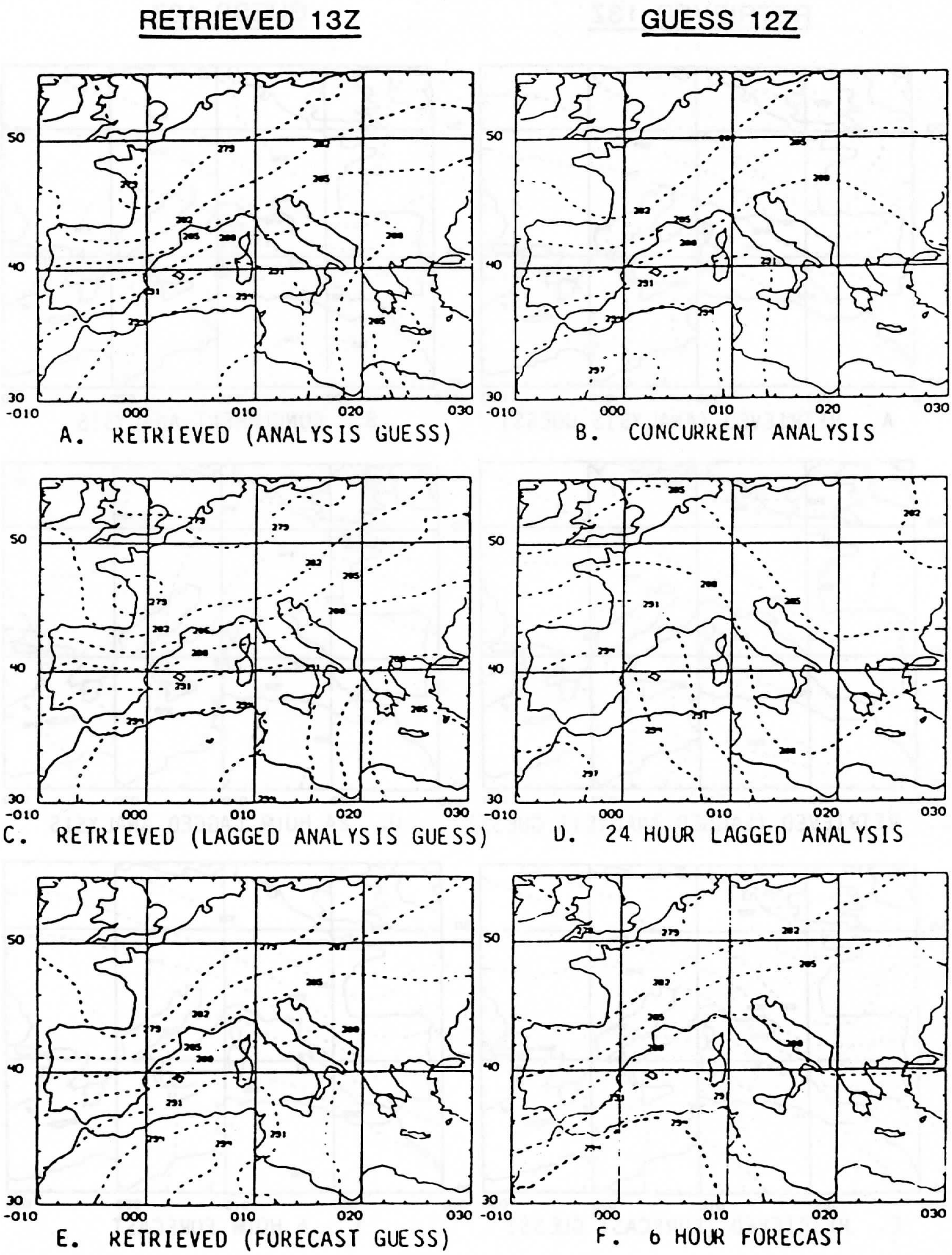


**Figure 1**

## 500-1000 MB THICKNESS MARCH 4, 1982

RETRIEVED 13Z — GUESS 12Z

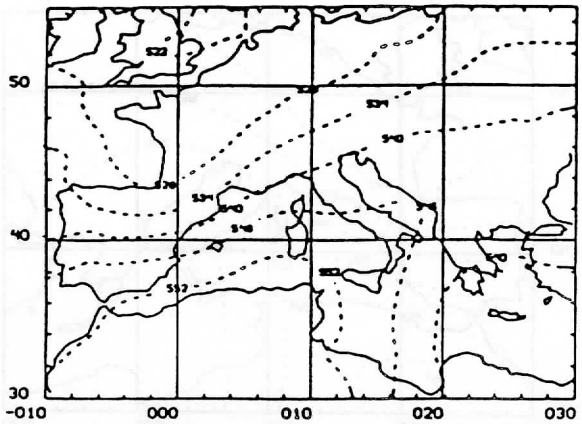


A. RETRIEVED (ANALYSIS GUESS)

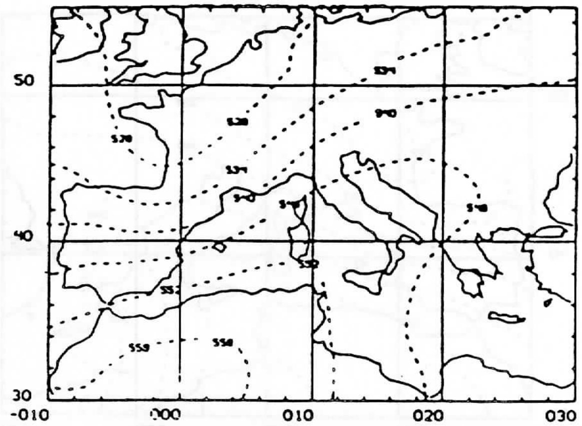


B. CONCURRENT ANALYSIS

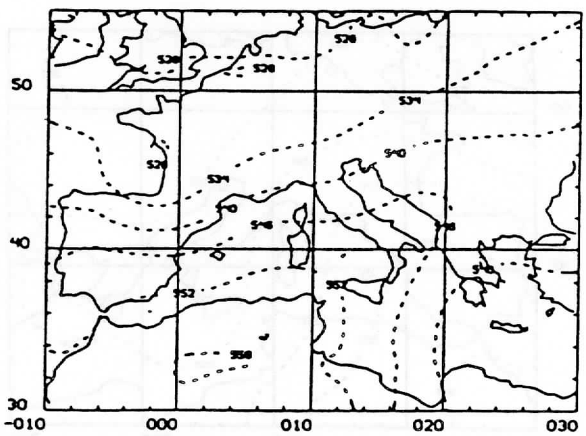


C. RETRIEVED (LAGGED ANALYSIS GUESS)

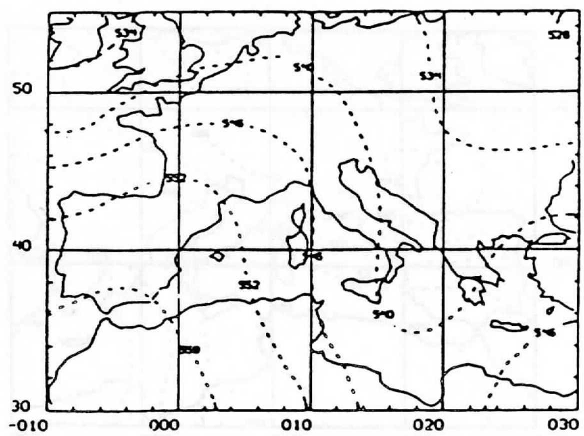


D. 24 HOUR LAGGED ANALYSIS

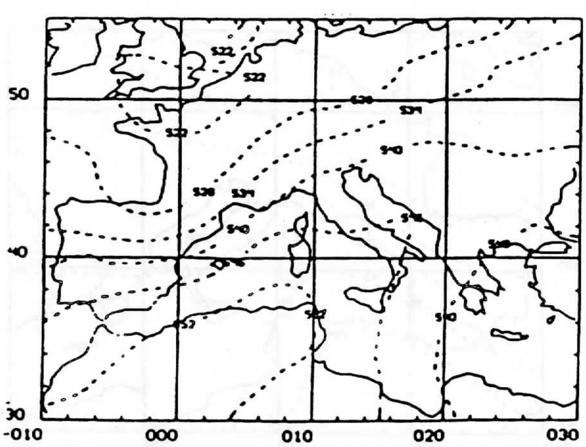


E. RETRIEVED (FORECAST GUESS)

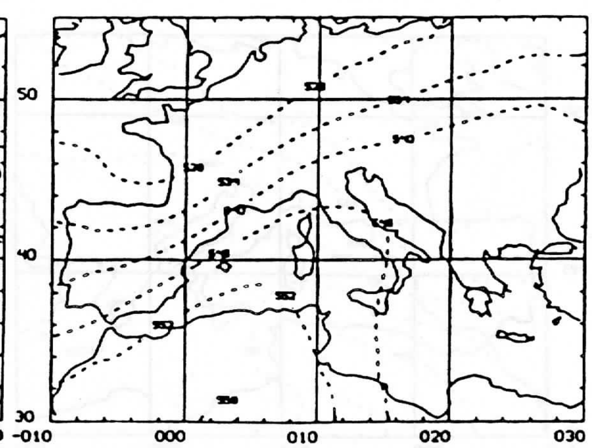


F. 6 HOUR FORECAST

Figure 2

## 500-700 MB THICKNESS MARCH 4, 1982

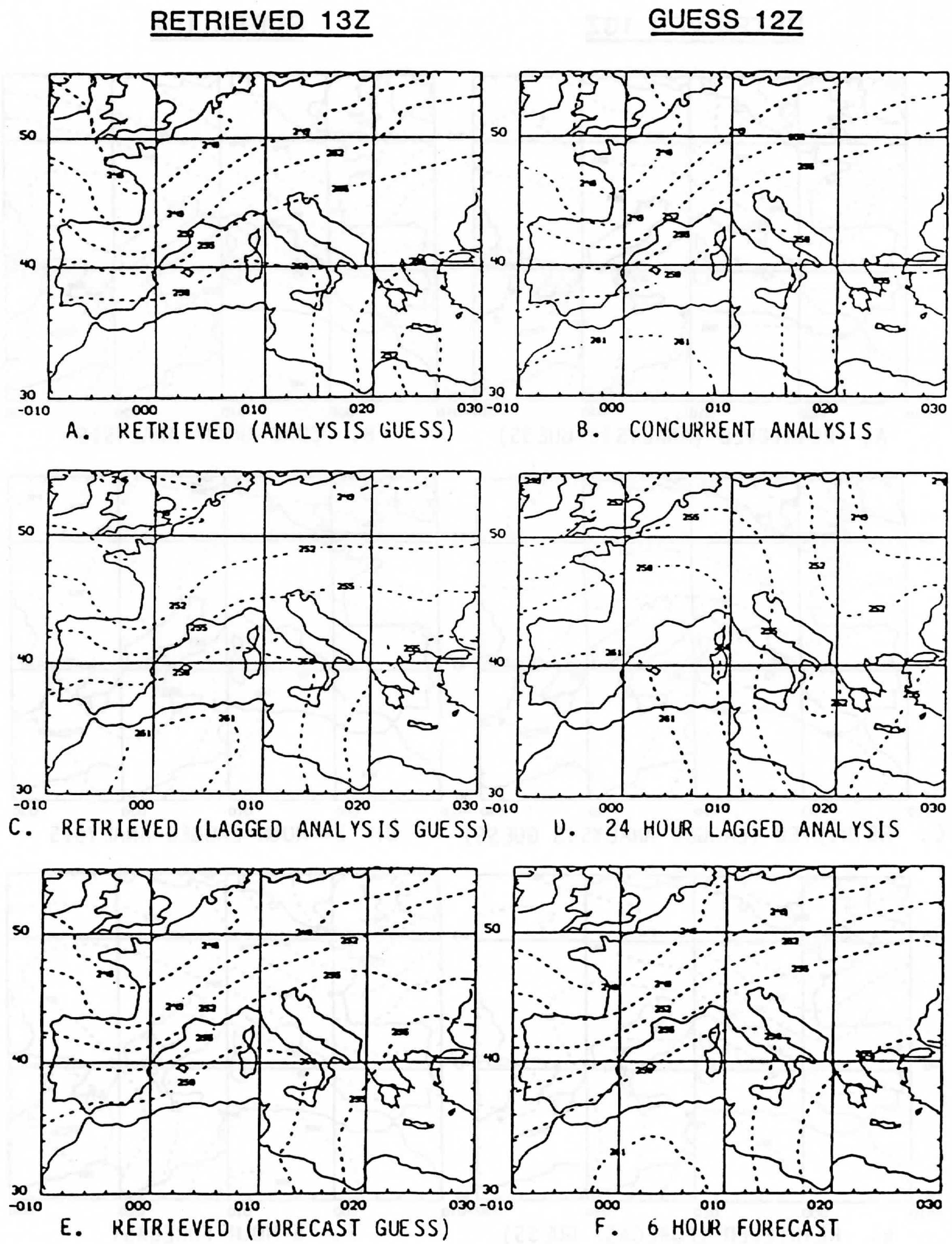


Figure 3

## 300-500 MB THICKNESS MARCH 4, 1982

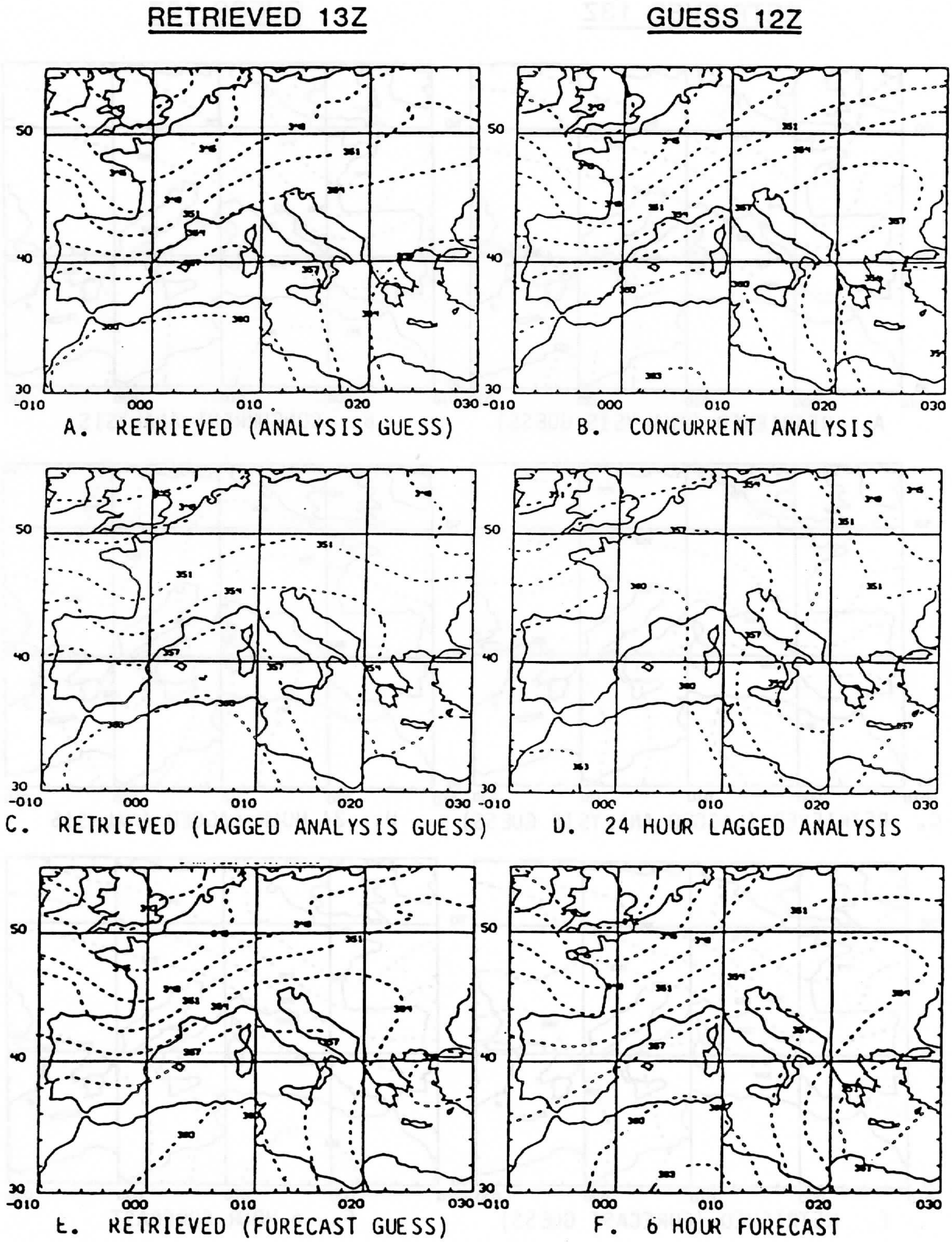


Figure 4

## 100-300 MB THICKNESS MARCH 4, 1982

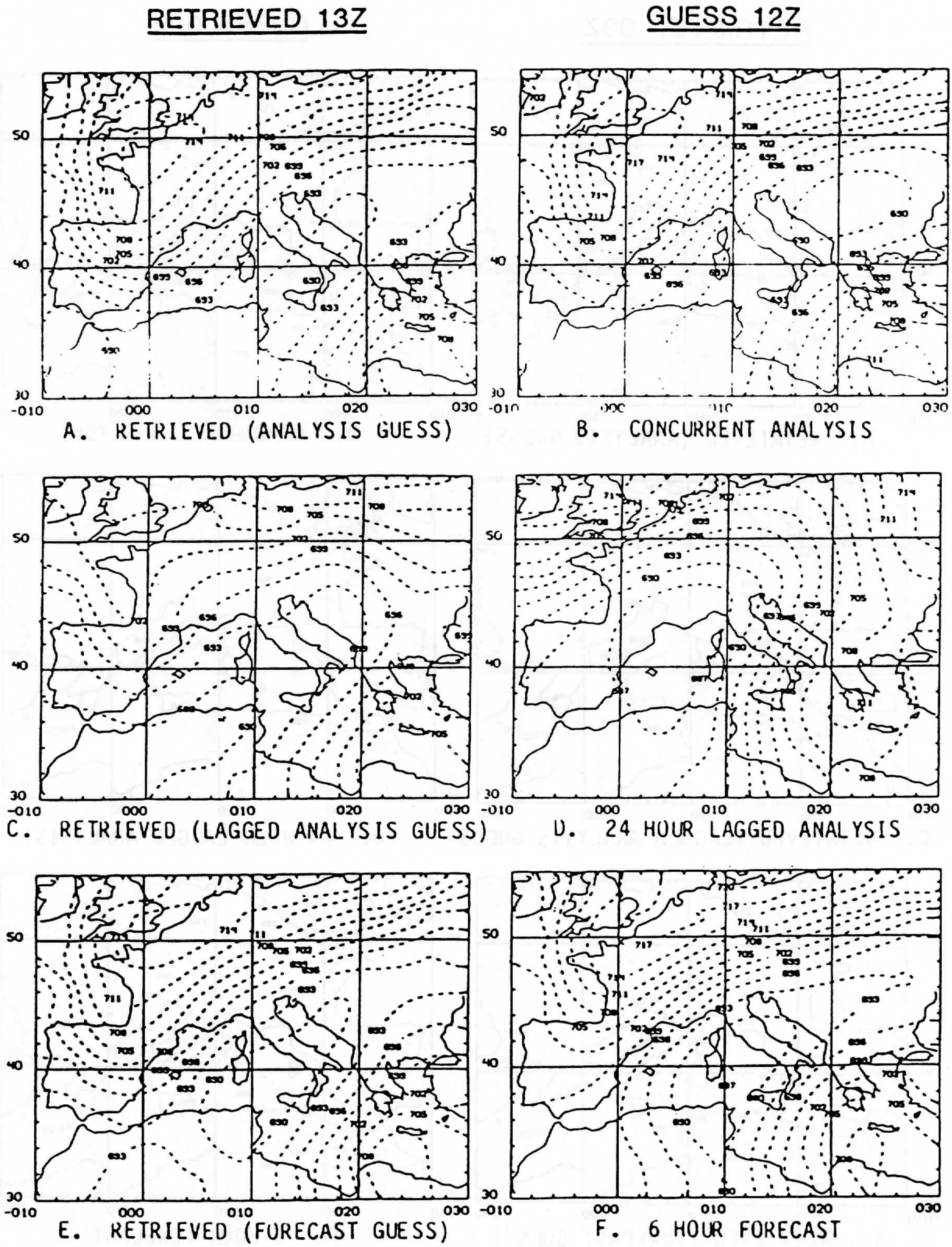


Figure 5

## 700-1000 MB THICKNESS MARCH 5, 1982

RETRIEVED 03Z | GUESS 00Z

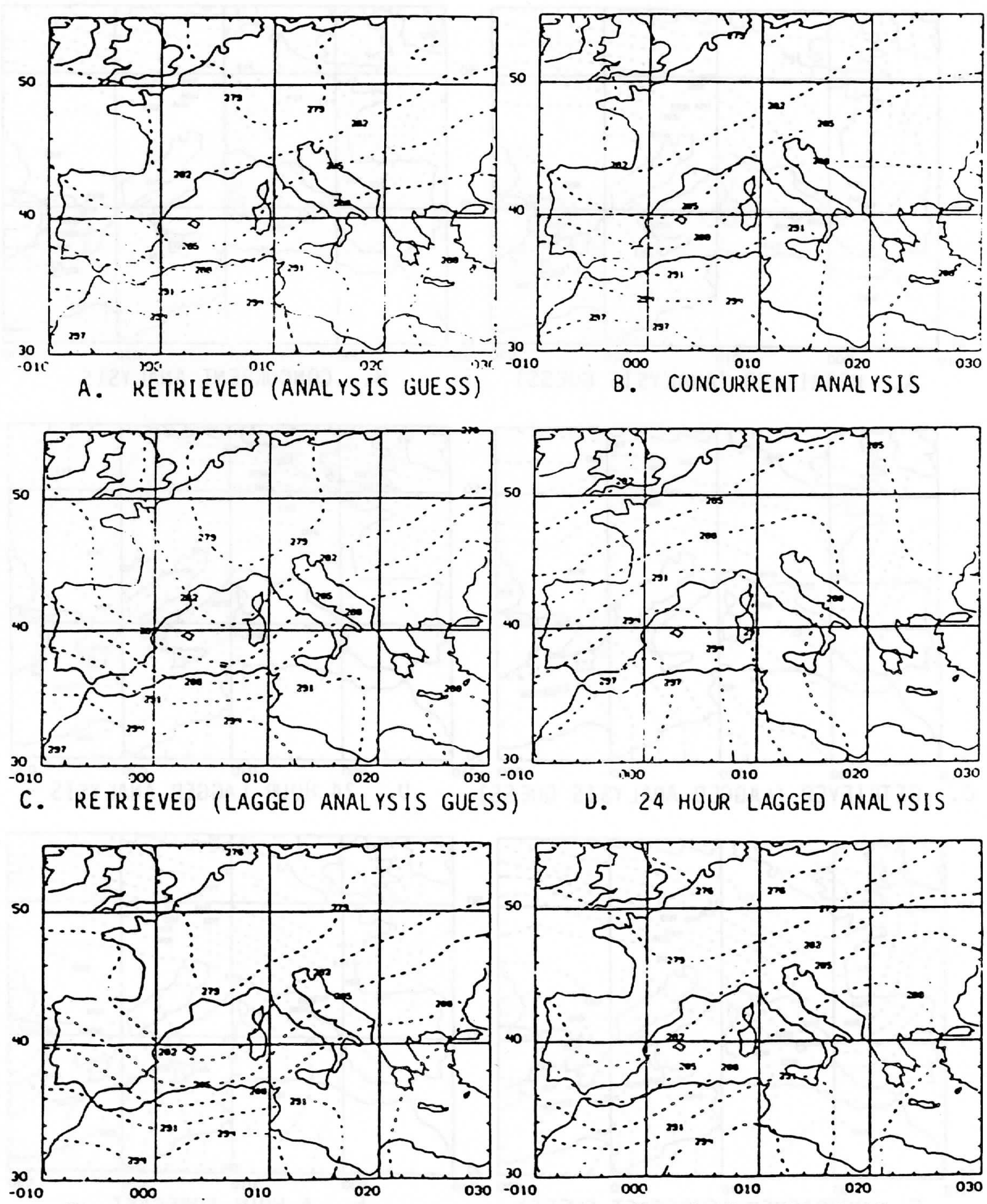

A. RETRIEVED (ANALYSIS GUESS)

B. CONCURRENT ANALYSIS

C. RETRIEVED (LAGGED ANALYSIS GUESS)

D. 24 HOUR LAGGED ANALYSIS

E. RETRIEVED (FORECAST GUESS)

F. 6 HOUR FORECAST

Figure 6

## 500-1000 MB THICKNESS MARCH 5, 1982

RETRIEVED 03Z GUESS 00Z

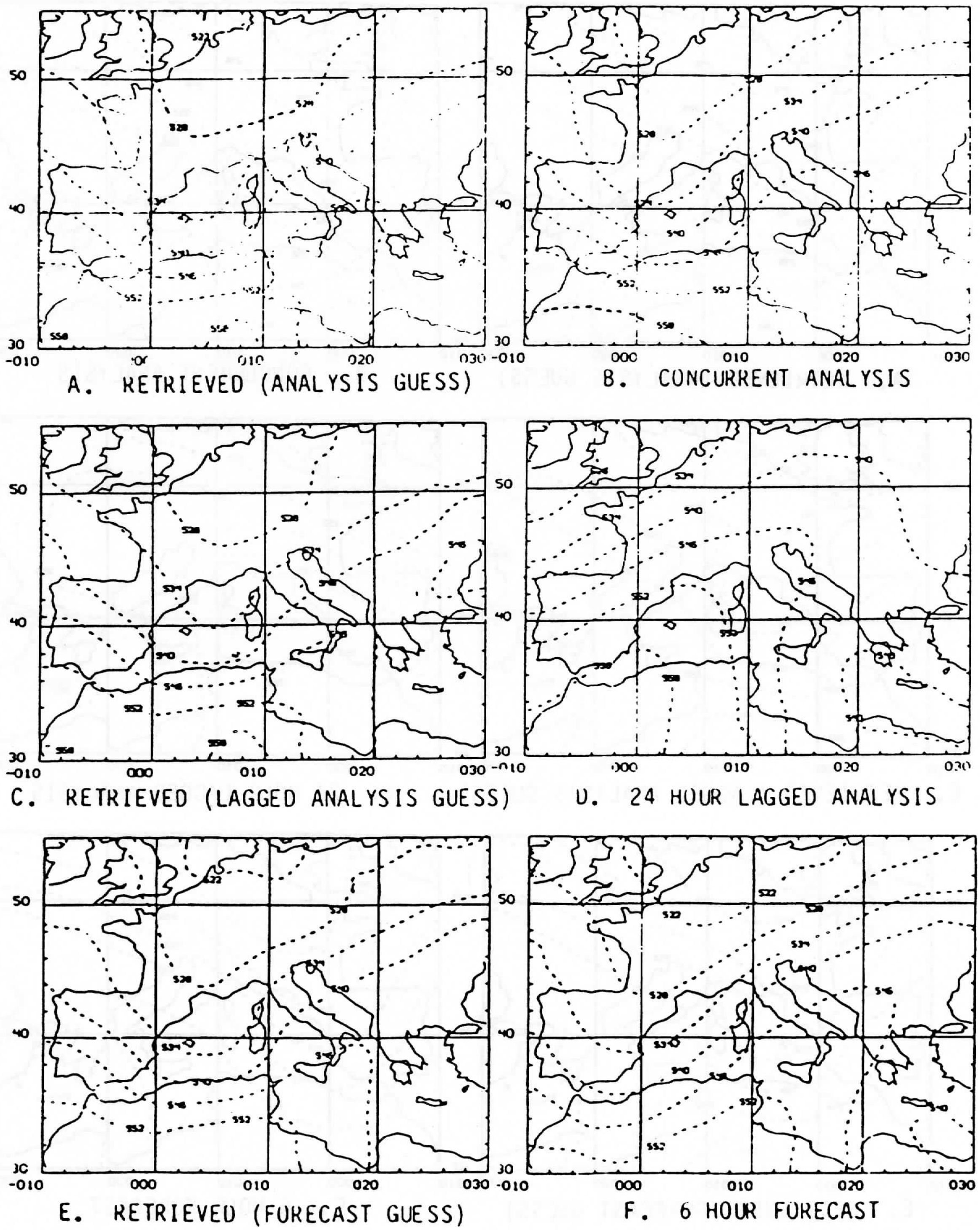


**Figure 7**

## 500-700 MB THICKNESS MARCH 5, 1982

RETRIEVED 03Z — GUESS 00Z

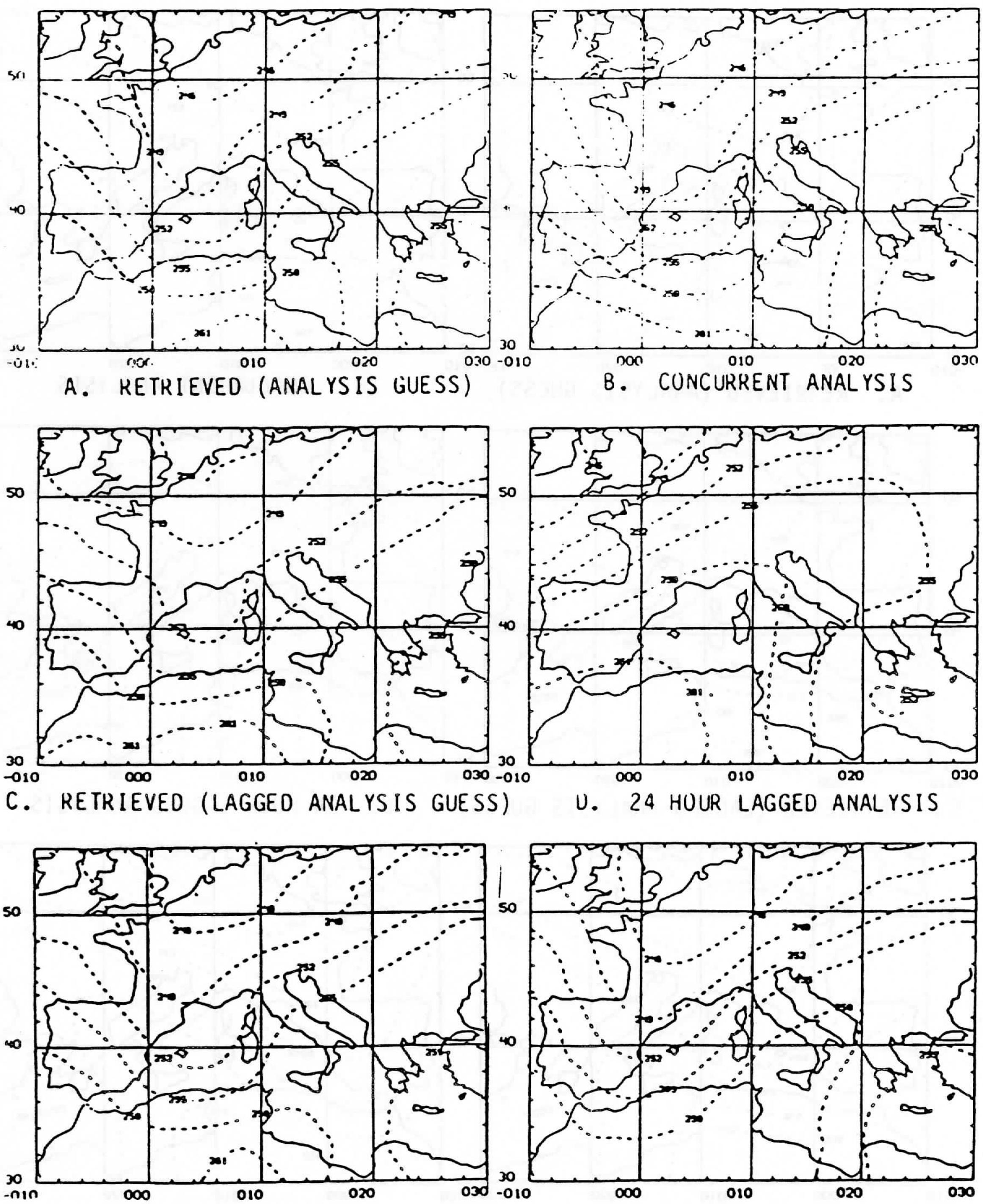


A. RETRIEVED (ANALYSIS GUESS)

B. CONCURRENT ANALYSIS

C. RETRIEVED (LAGGED ANALYSIS GUESS)

D. 24 HOUR LAGGED ANALYSIS

E. RETRIEVED (FORECAST GUESS)

F. 6 HOUR FORECAST

**Figure 8**

## 300-500 MB THICKNESS MARCH 5, 1982

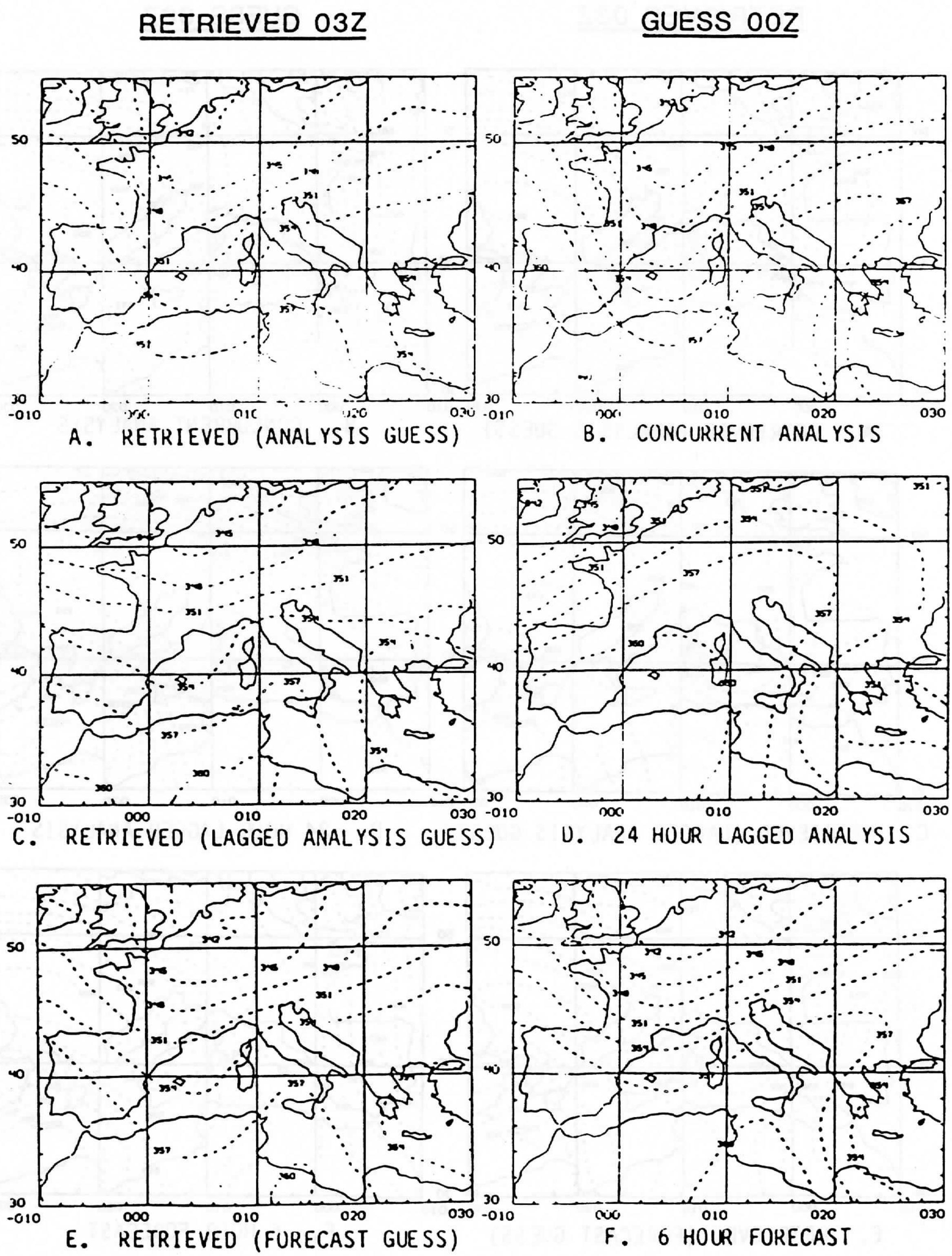


**Figure 9**

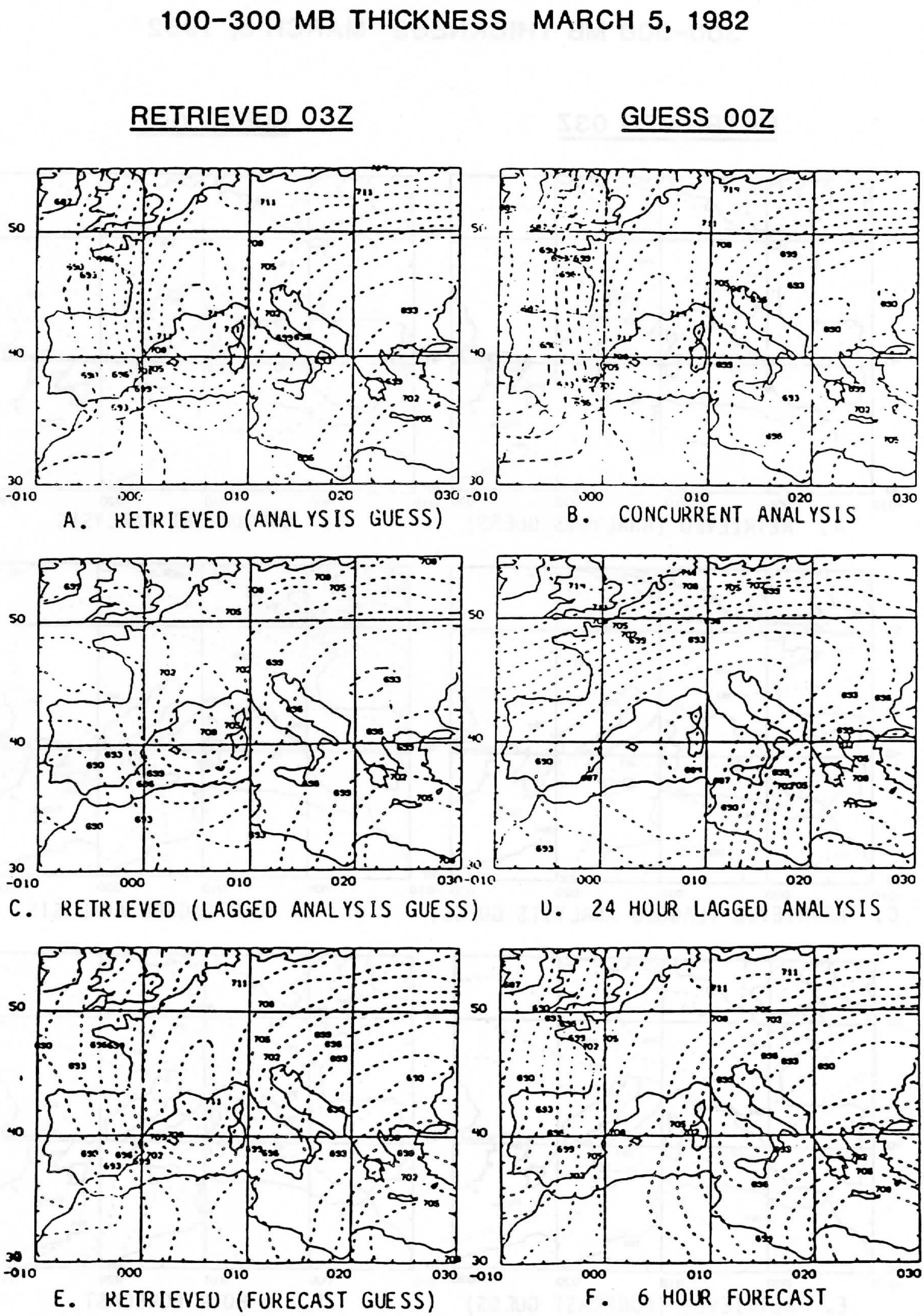
100-300 MB THICKNESS MARCH 5, 1982
RETRIEVED 03Z
GUESS 00Z
A. RETRIEVED (ANALYSIS GUESS)
B. CONCURRENT ANALYSIS
C. RETRIEVED (LAGGED ANALYSIS GUESS)
D. 24 HOUR LAGGED ANALYSIS
E. RETRIEVED (FORECAST GUESS)
F. 6 HOUR FORECAST

Figure 10

## PRECIPITABLE WATER 1000 MB-TOP MARCH 4, 1982 (G/CM$^2$)

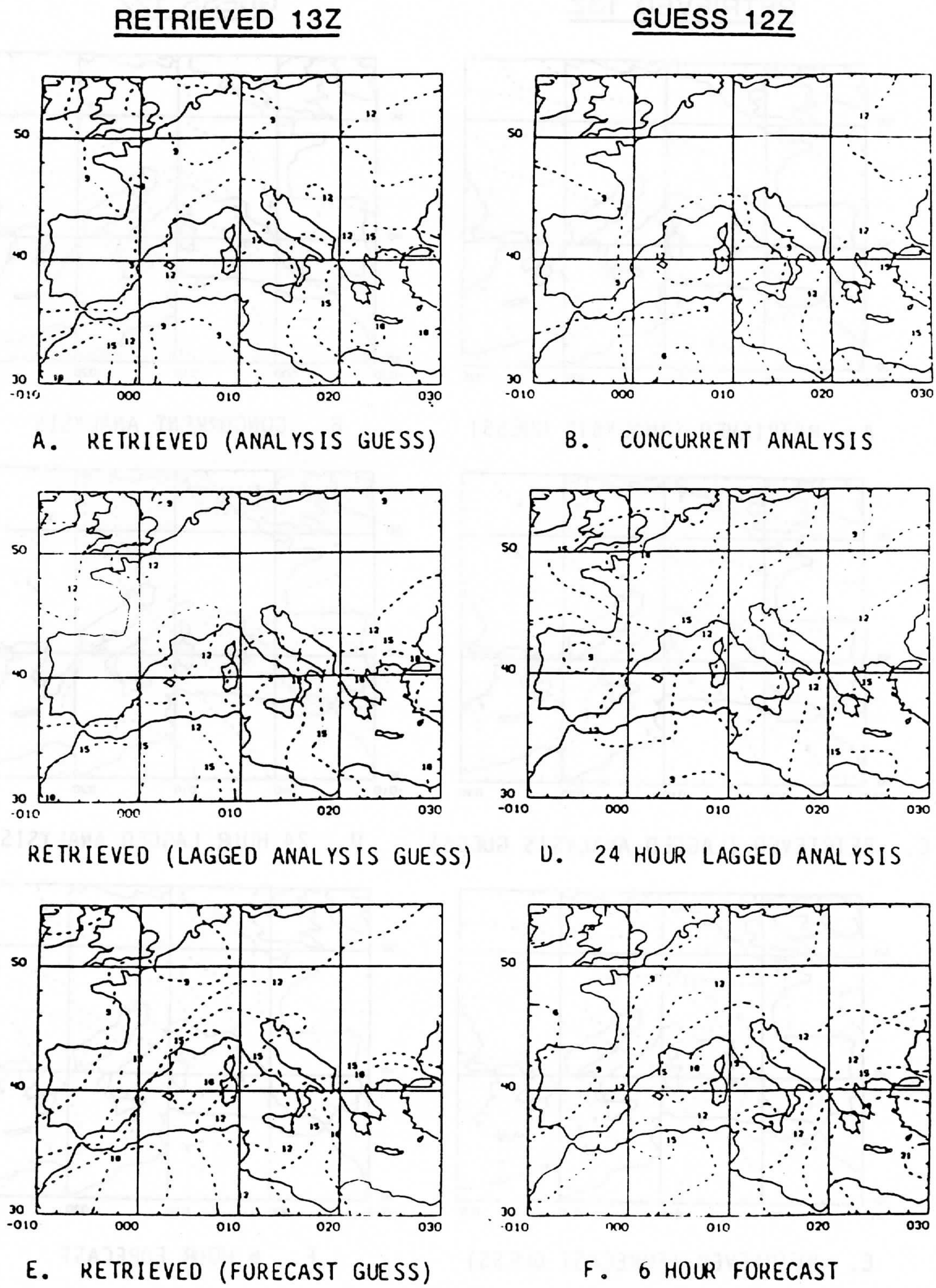


**Figure 11**

## PRECIPITABLE WATER 700 MB-TOP MARCH 4, 1982 (G/CM$^2$ x 10)

**RETRIEVED 13Z** | **GUESS 12Z**

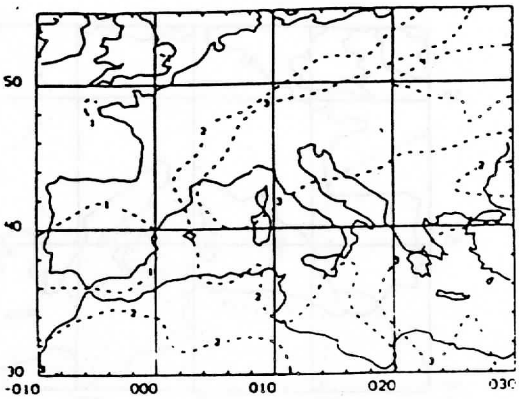


A. RETRIEVED (ANALYSIS GUESS)

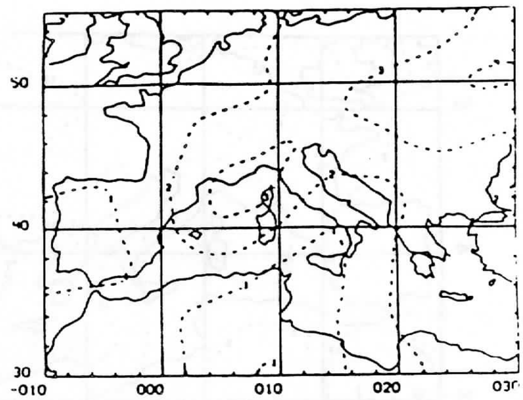


B. CONCURRENT ANALYSIS

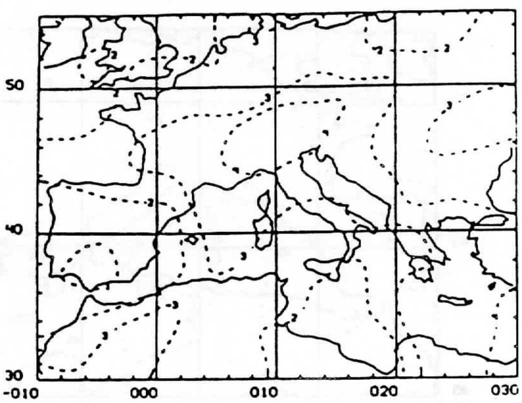


C. RETRIEVED (LAGGED ANALYSIS GUESS)

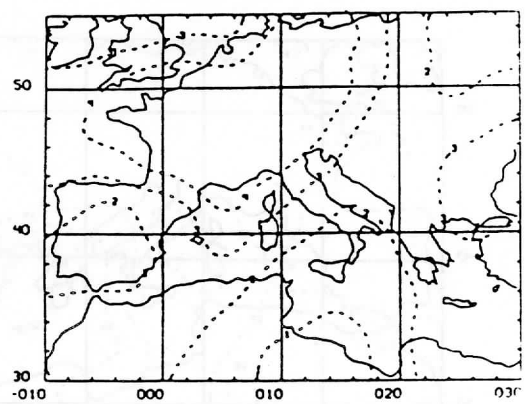


D. 24 HOUR LAGGED ANALYSIS

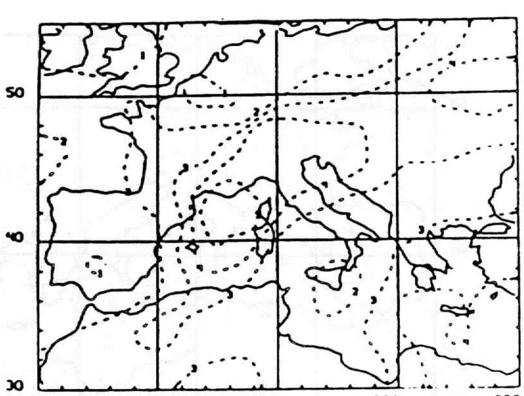


E. RETRIEVED (FORECAST GUESS)

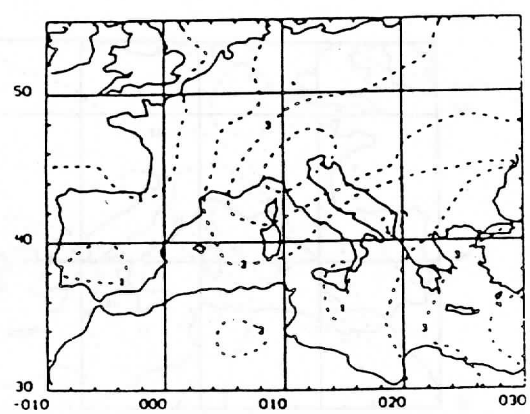


F. 6 HOUR FORECAST

**Figure 12**

## PRECIPITABLE WATER 500 MB-TOP MARCH 4, 1982 ($G/CM^2 \times 100$)

RETRIEVED 13Z | GUESS 12Z

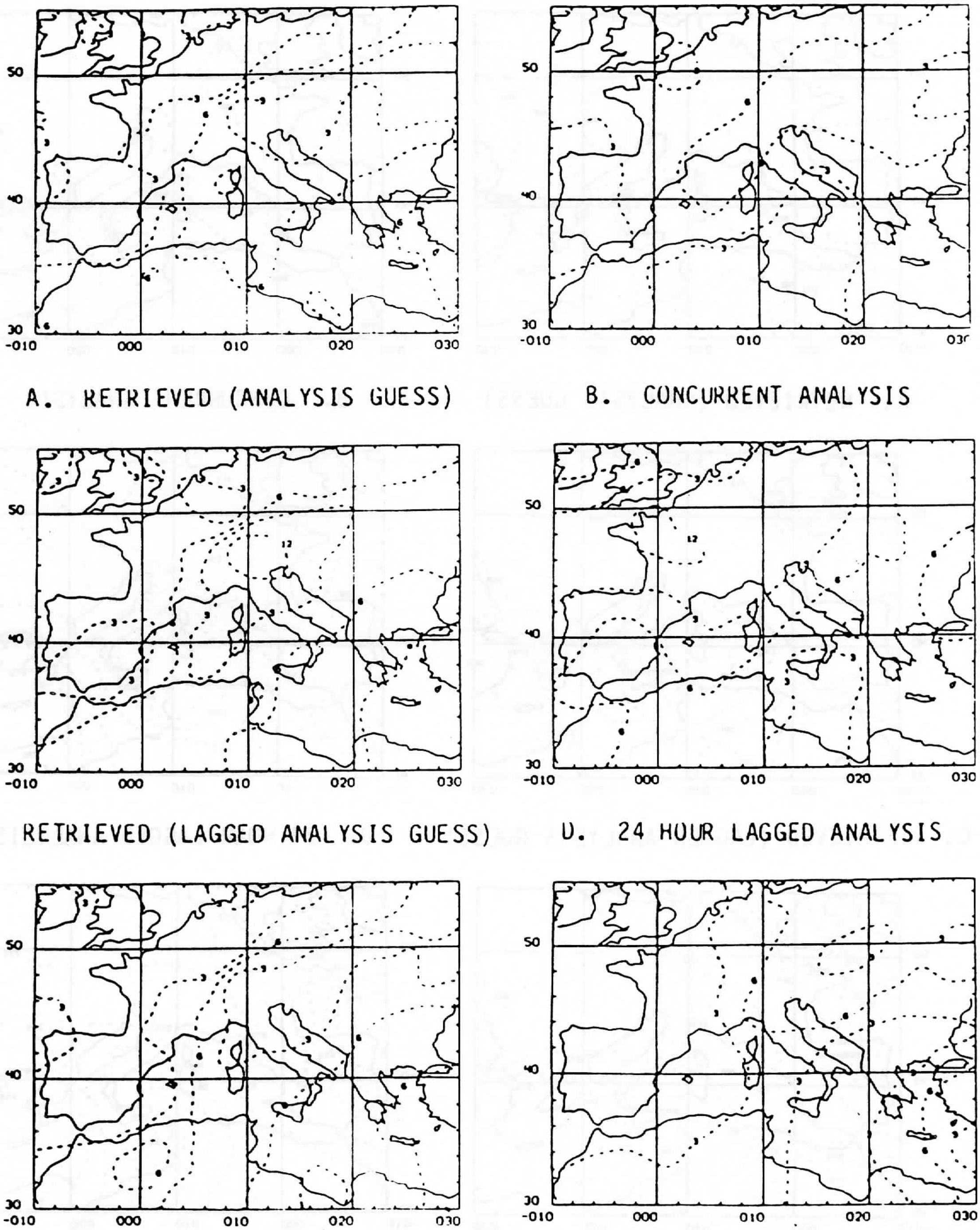


A. RETRIEVED (ANALYSIS GUESS)

B. CONCURRENT ANALYSIS

C. RETRIEVED (LAGGED ANALYSIS GUESS)

D. 24 HOUR LAGGED ANALYSIS

E. RETRIEVED (FORECAST GUESS)

F. 6 HOUR FORECAST

**Figure 13**

# DEW POINT 850 MB MARCH 4, 1982

**RETRIEVED 13Z** | **GUESS 12Z**

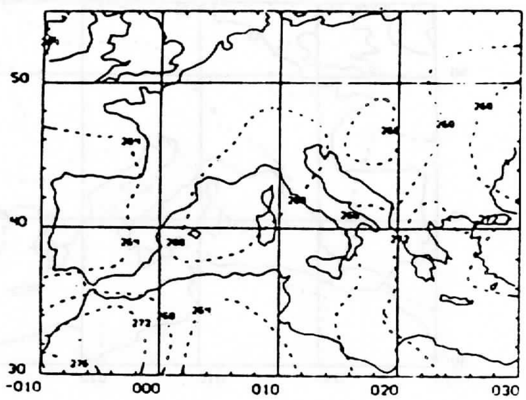


A. RETRIEVED (ANALYSIS GUESS)

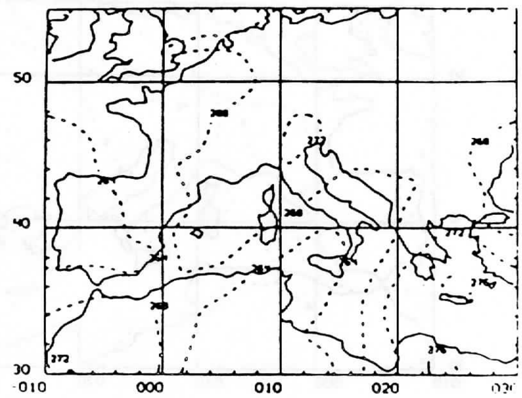


B. CONCURRENT ANALYSIS

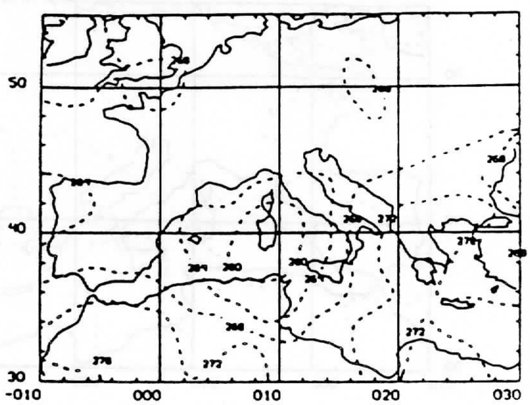


C. RETRIEVED (LAGGED ANALYSIS GUESS)

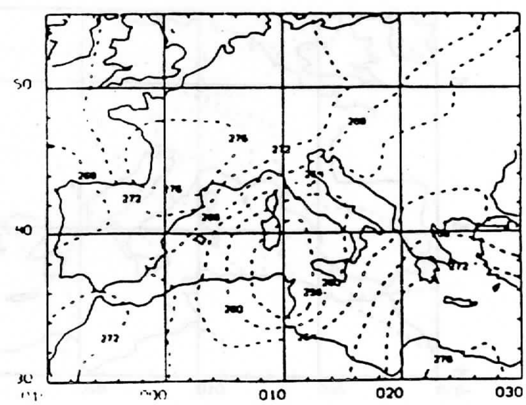


D. 24 HOUR LAGGED ANALYSIS

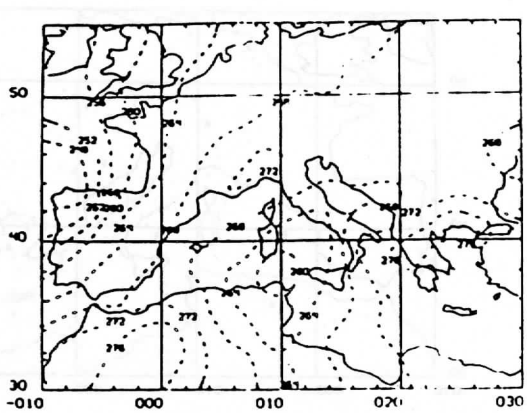


E. RETRIEVED (FORECAST GUESS)

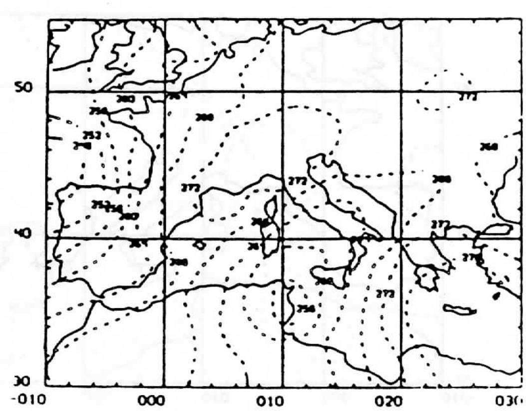


F. 6 HOUR FORECAST

**Figure 14**

## DEW POINT 700 MB MARCH 4, 1982

RETRIEVED 13Z — GUESS 12Z

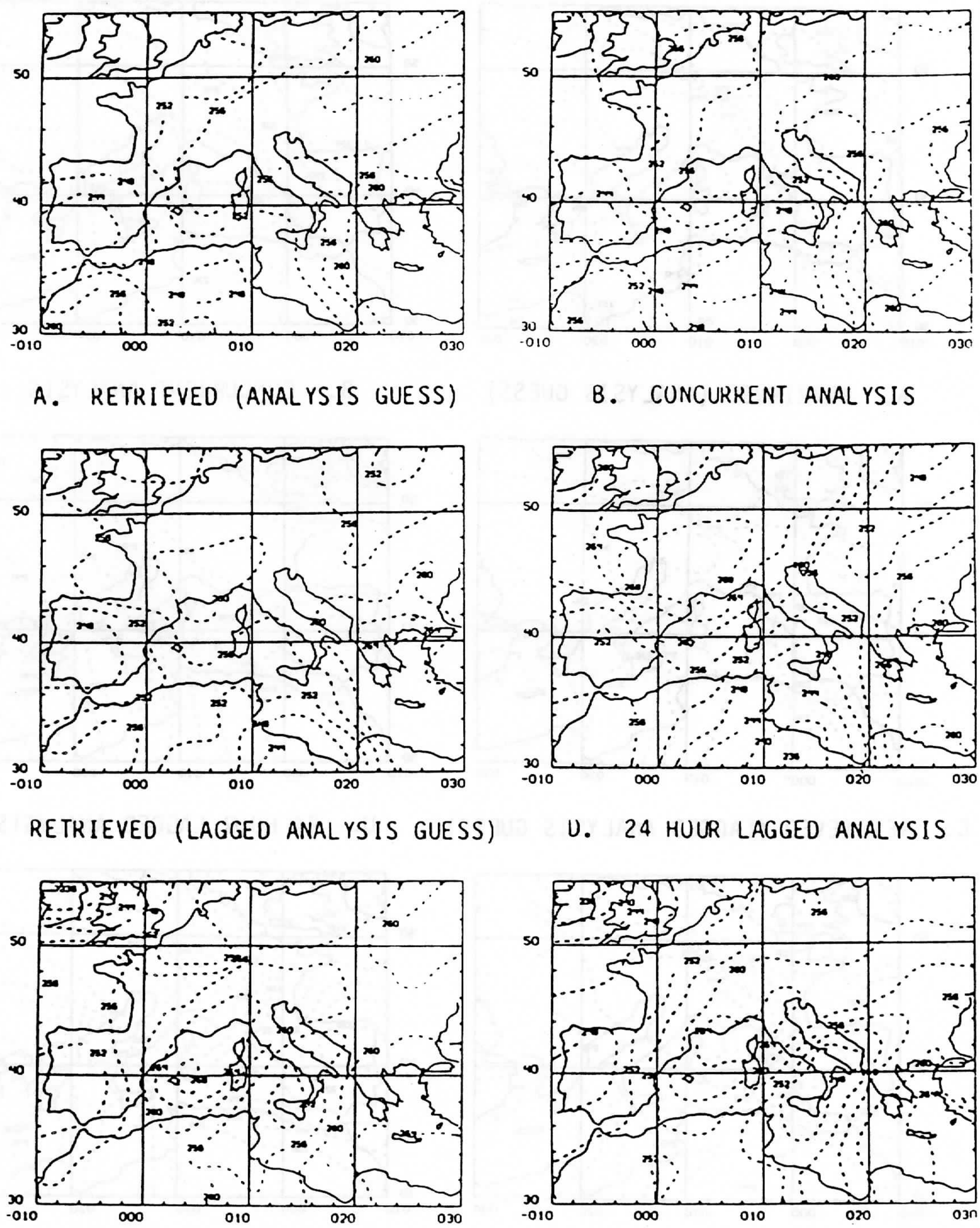

A. RETRIEVED (ANALYSIS GUESS)

B. CONCURRENT ANALYSIS

C. RETRIEVED (LAGGED ANALYSIS GUESS)

D. 24 HOUR LAGGED ANALYSIS

E. RETRIEVED (FORECAST GUESS)

F. 6 HOUR FORECAST

**Figure 15**

## DEW POINT 500 MB MARCH 4, 1982

**RETRIEVED 13Z** — **GUESS 12Z**

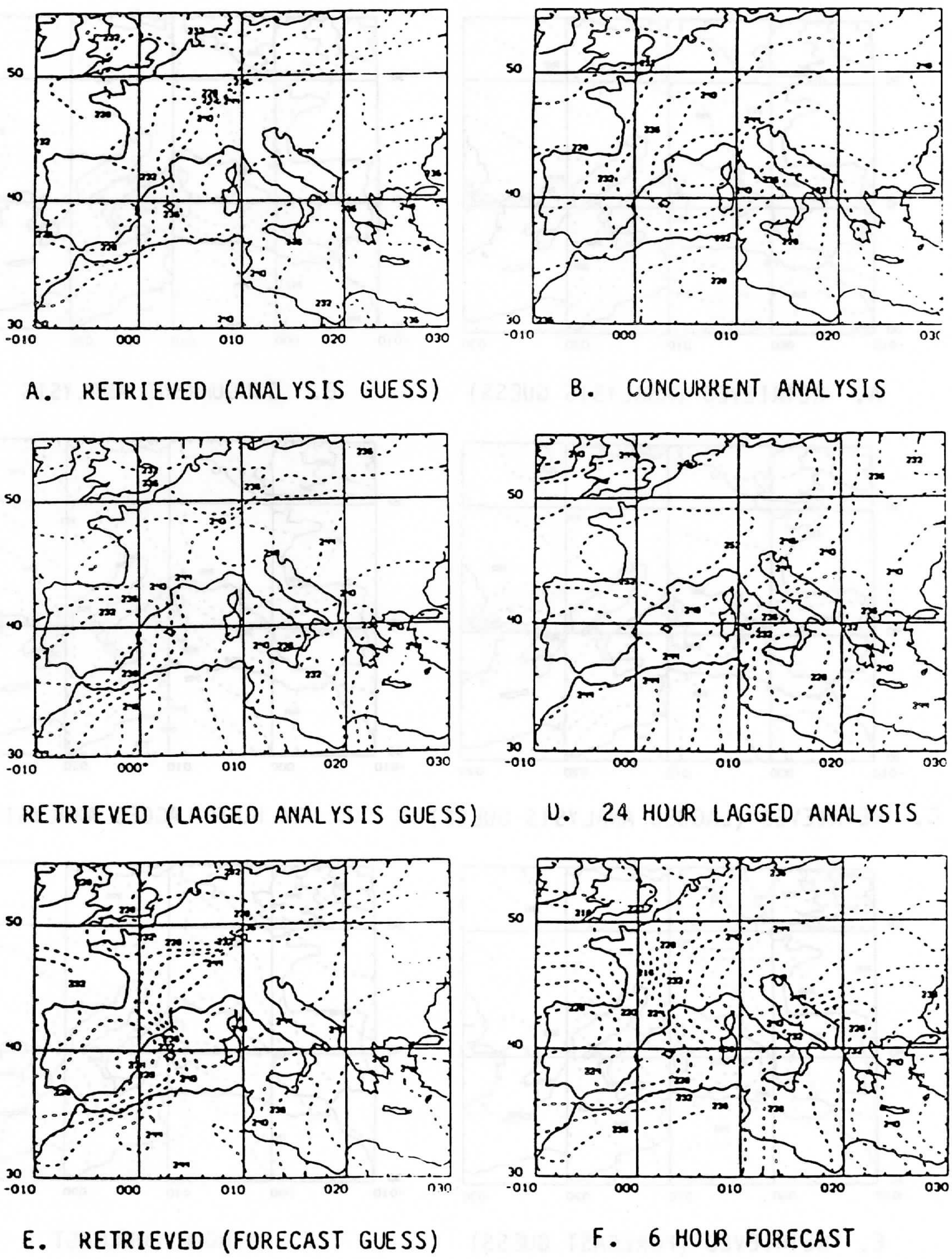

A. RETRIEVED (ANALYSIS GUESS)

B. CONCURRENT ANALYSIS

C. RETRIEVED (LAGGED ANALYSIS GUESS)

D. 24 HOUR LAGGED ANALYSIS

E. RETRIEVED (FORECAST GUESS)

F. 6 HOUR FORECAST

Figure 16

## PRECIPITABLE WATER 1000 MB–TOP MARCH 5, 1982 (G/CM$^2$)

**RETRIEVED 03Z** | **GUESS 00Z**

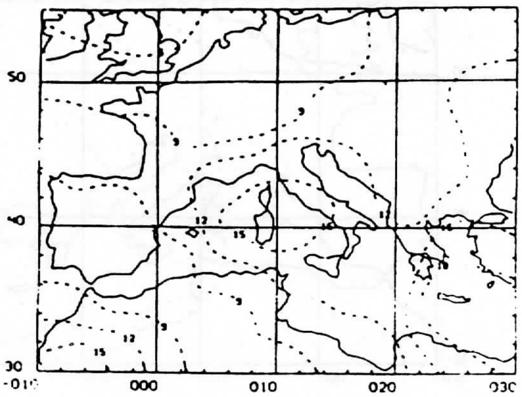


A. RETRIEVED (ANALYSIS GUESS)

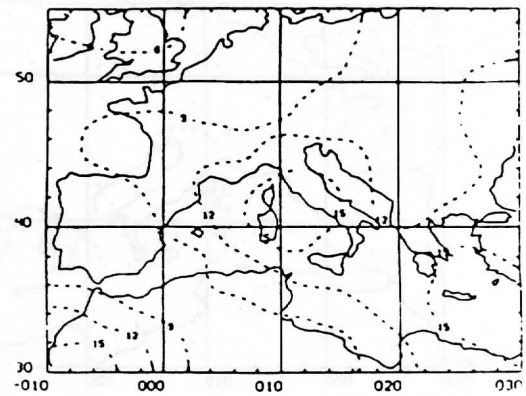


B. CONCURRENT ANALYSIS

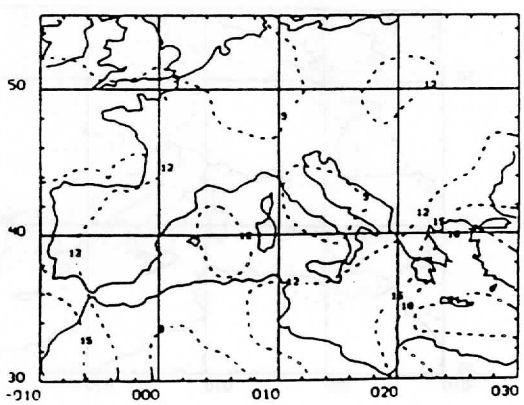


C. RETRIEVED (LAGGED ANALYSIS GUESS)

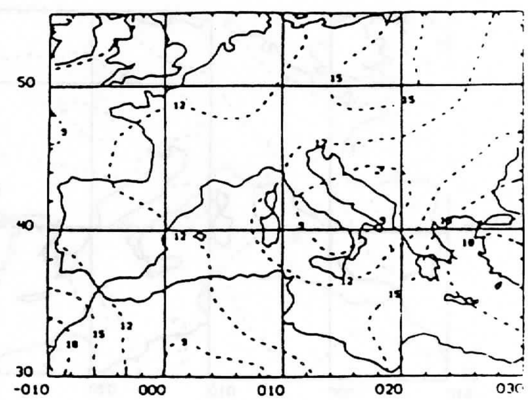


D. 24 HOUR LAGGED ANALYSIS

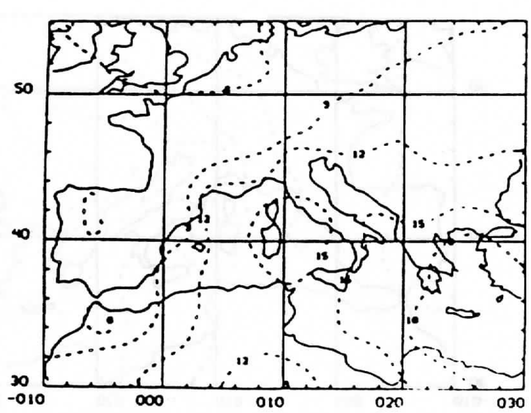


E. RETRIEVED (FORECAST GUESS)

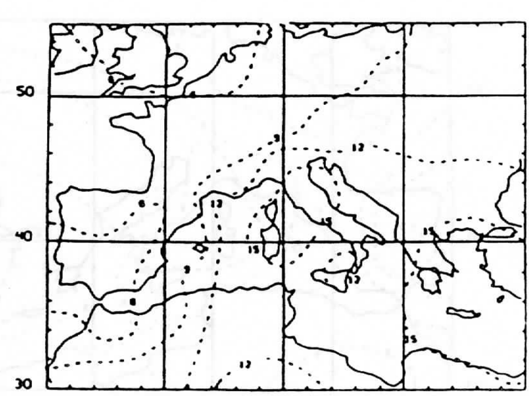


F. 6 HOUR FORECAST

**Figure 17**

## PRECIPITABLE WATER 700 MB-TOP MARCH 5, 1982 ($G/CM^2$ x 10)

### RETRIEVED 03Z

### GUESS 00Z

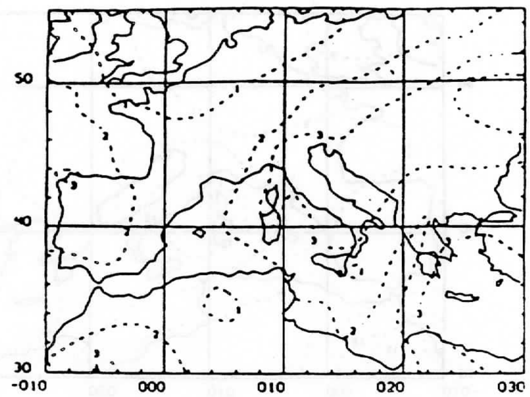


A. RETRIEVED (ANALYSIS GUESS)

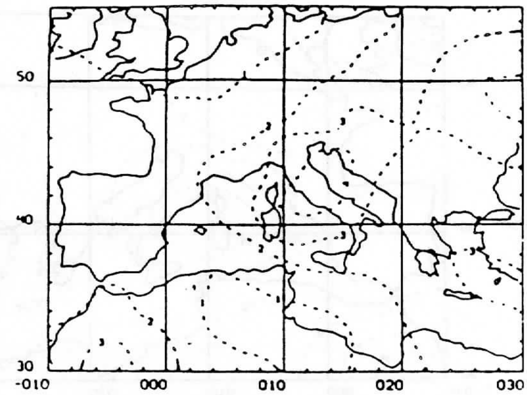


B. CONCURRENT ANALYSIS

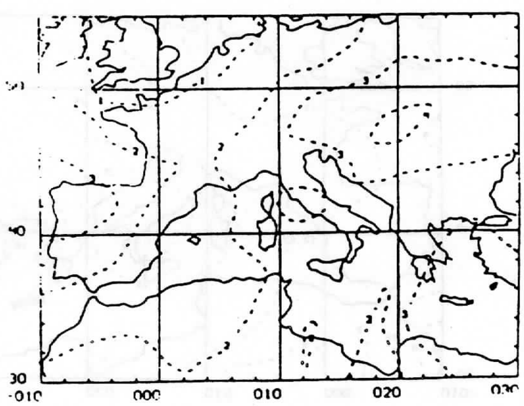


C. RETRIEVED (LAGGED ANALYSIS GUESS)

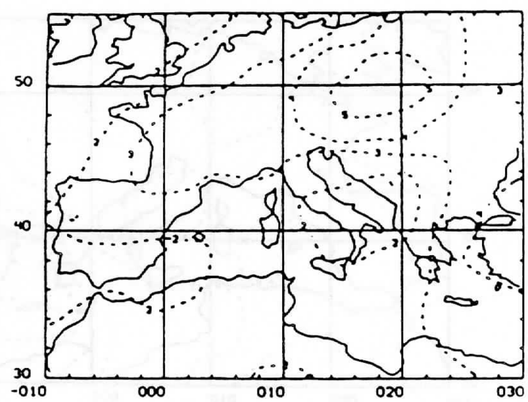


D. 24 HOUR LAGGED ANALYSIS

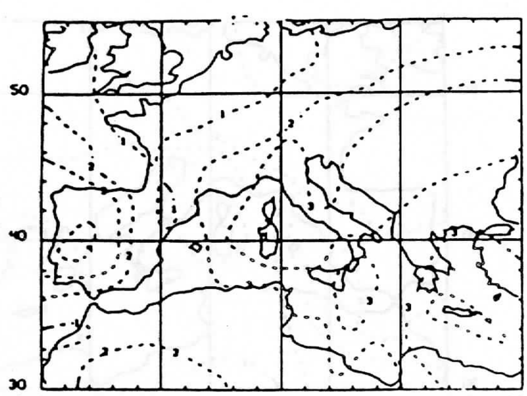


E. RETRIEVED (FORECAST GUESS)

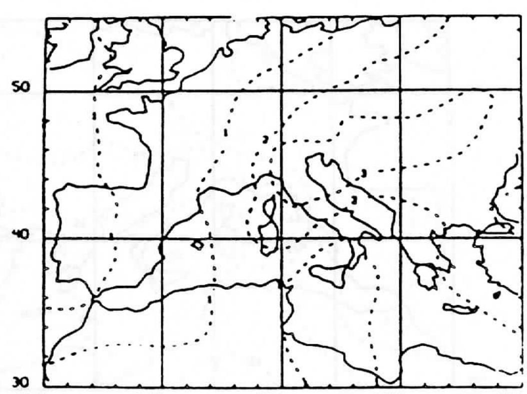


F. 6 HOUR FORECAST

**Figure 18**

## PRECIPITABLE WATER 500 MB-TOP MARCH 5, 1982 ($G/CM^2 \times 100$)

**RETRIEVED 03Z** | **GUESS 00Z**

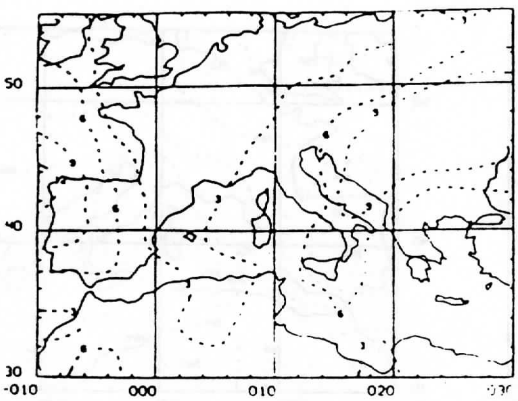


A. RETRIEVED (ANALYSIS GUESS)

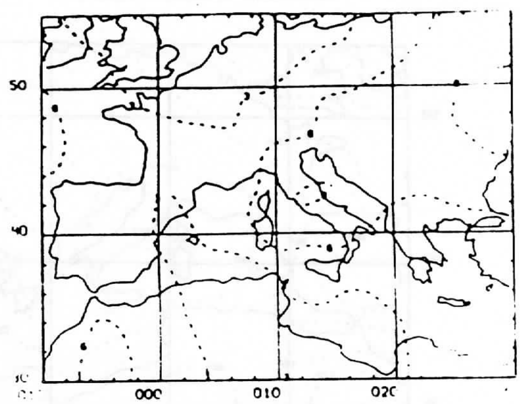


B. CONCURRENT ANALYSIS

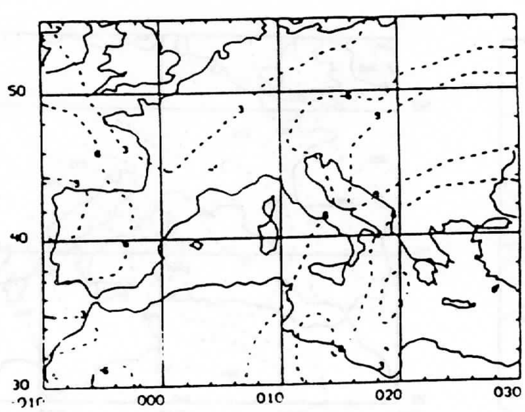


C. RETRIEVED (LAGGED ANALYSIS GUESS)

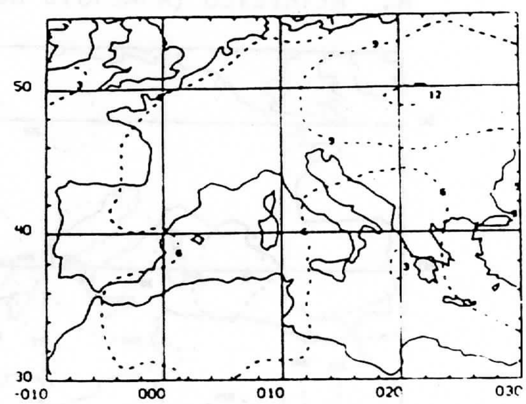


D. 24 HOUR LAGGED ANALYSIS

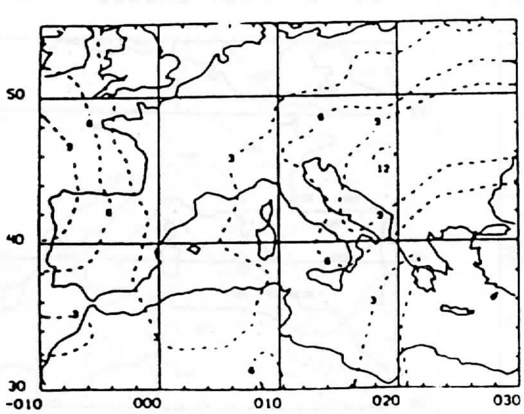


E. RETRIEVED (FORECAST GUESS)

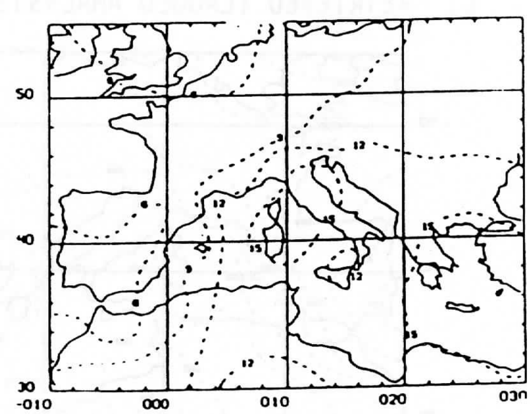


F. 6 HOUR FORECAST

**Figure 19**

## DEW POINT 850 MB  MARCH 5, 1982

**RETRIEVED 03Z** | **GUESS 00Z**

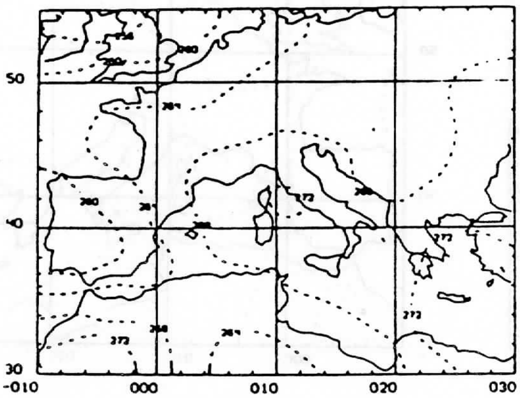


A. RETRIEVED (ANALYSIS GUESS)

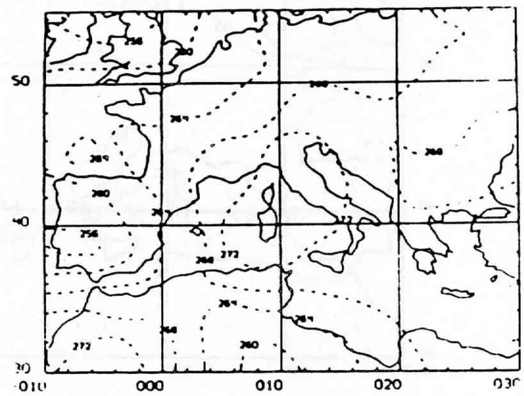


B. CONCURRENT ANALYSIS

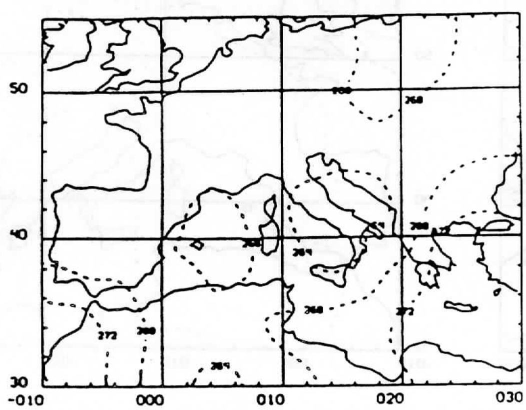


C. RETRIEVED (LAGGED ANALYSIS GUESS)

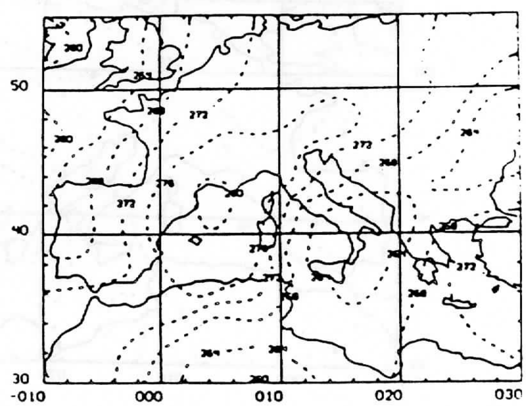


D. 24 HOUR LAGGED ANALYSIS

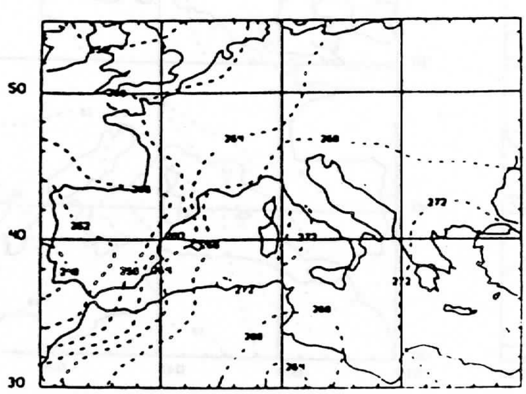


E. RETRIEVED (FORECAST GUESS)

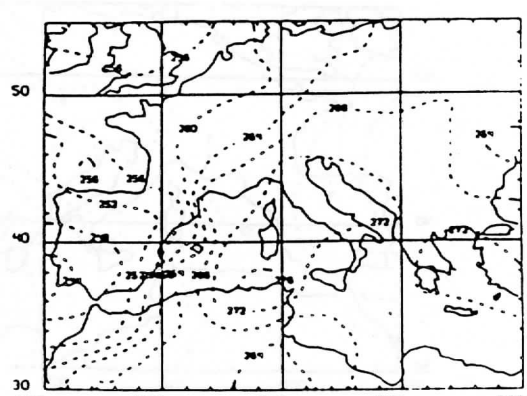


F. 6 HOUR FORECAST

**Figure 20**

# DEW POINT 700 MB MARCH 5, 1982

**RETRIEVED 03Z** | **GUESS 00Z**

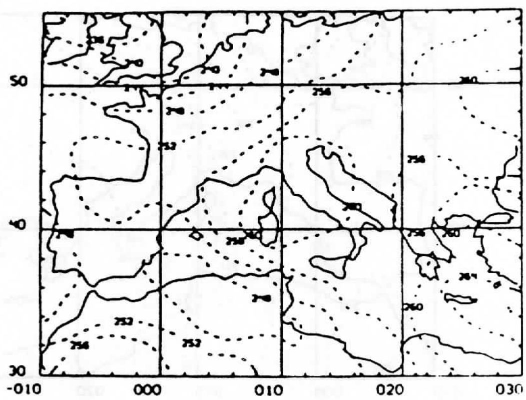


A. RETRIEVED (ANALYSIS GUESS)

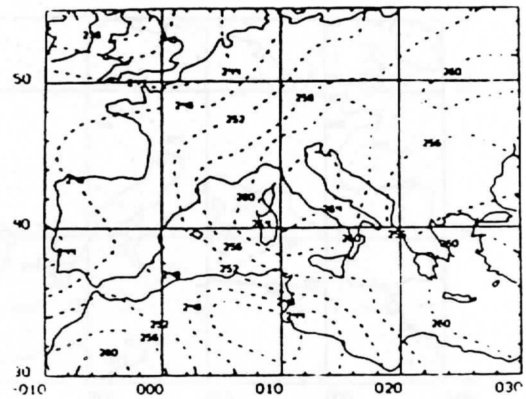


B. CONCURRENT ANALYSIS

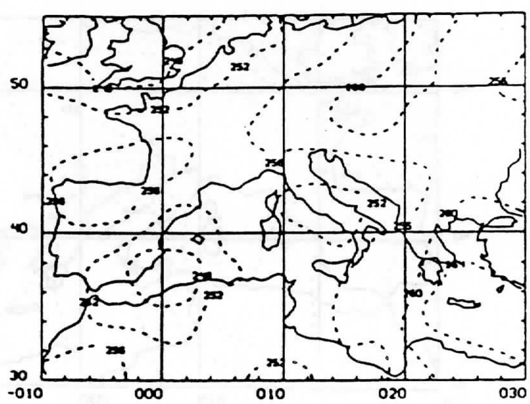


C. RETRIEVED (LAGGED ANALYSIS GUESS)

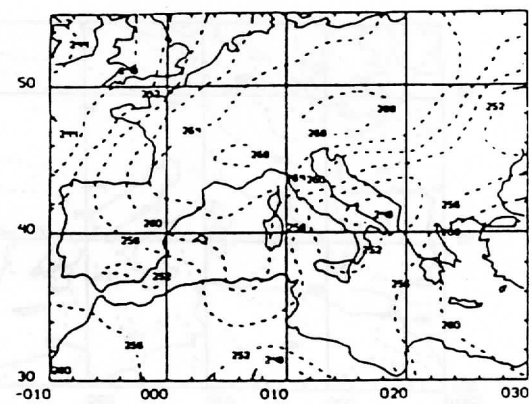


D. 24 HOUR LAGGED ANALYSIS

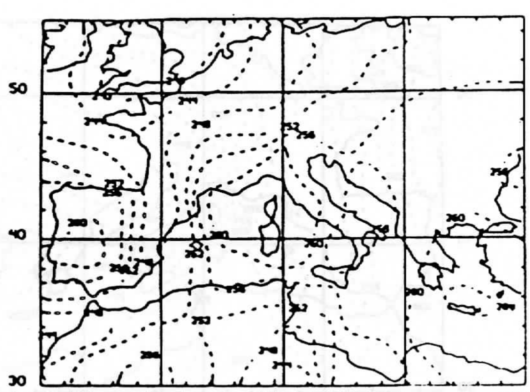


E. RETRIEVED (FORECAST GUESS)

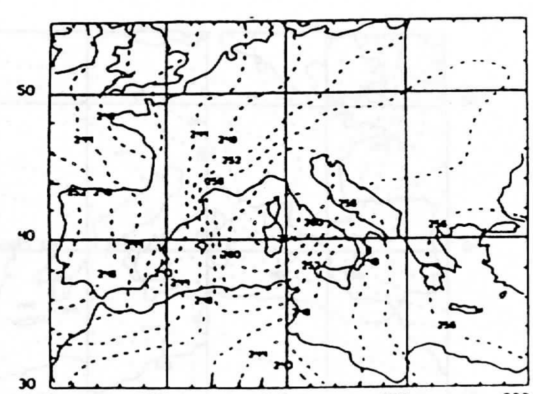


F. 6 HOUR FORECAST

**Figure 21**

# DEW POINT 500MB MARCH 5, 1982

RETRIEVED 03Z | GUESS 00Z

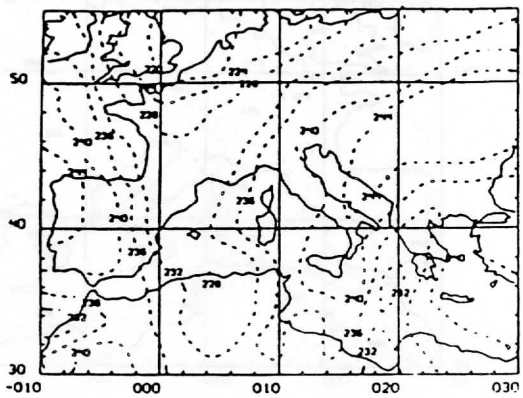


A. RETRIEVED (ANALYSIS GUESS)

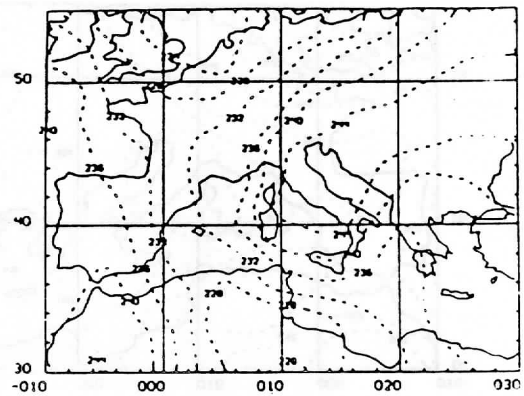


B. CONCURRENT ANALYSIS

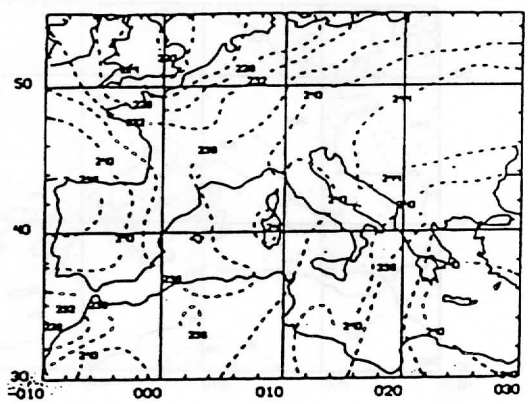


C. RETRIEVED (LAGGED ANALYSIS GUESS)

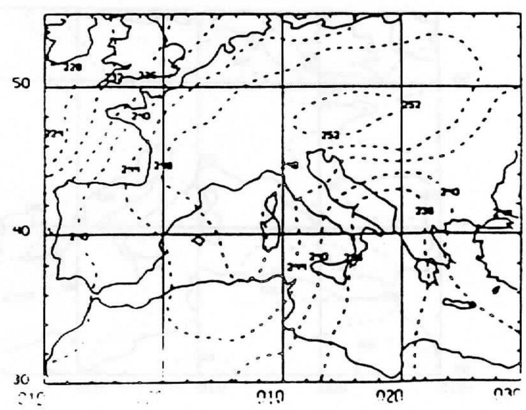


D. 24 HOUR LAGGED ANALYSIS

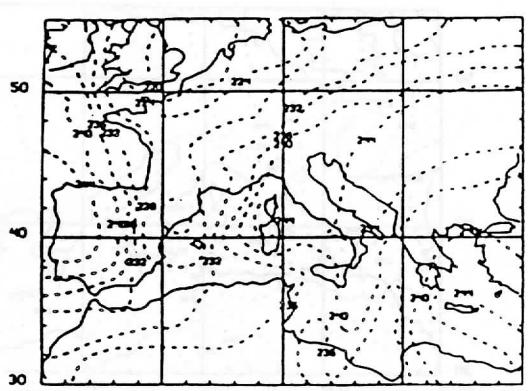


E. RETRIEVED (FORECAST GUESS)

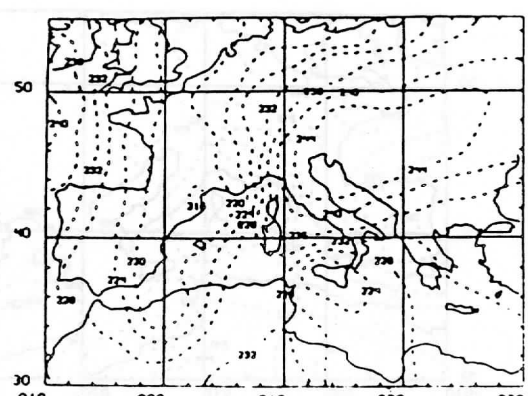


F. 6 HOUR FORECAST

Figure 22

# The Technical Proceedings of
# The Second International TOVS Study Conference

**Igls, Austria**

**February 18 - 22, 1985**

**Edited by**

**W. P. Menzel**

**Cooperative Institute for Meteorological Satellite Studies**
**Space Science and Engineering Center**
**University of Wisconsin**
**1225 West Dayton Street**
**Madison, Wisconsin 53706**
**(608)262-0544**

**September 1985**